

**Propagation of Price Shocks
to CPI Inflation**

The Role of Cross-demand
Dependencies

Christian Glocker
Philipp Piribauer

Propagation of Price Shocks to CPI Inflation

The Role of Cross-demand Dependencies

Christian Glocker, Philipp Piribauer

WIFO Working Papers 663/2023

July 2023

Abstract

Cross-demand creates links between goods which cause demand-driven cross-price dependencies. We construct a theoretical model to analyze their role in propagating microeconomic price shocks to the CPI inflation rate and examine their empirical relevance using spatial econometric techniques. The results highlight the importance of complementarity and substitution properties between goods in exacerbating or mitigating price shocks. This contrasts with the propagation through the production network. Most importantly, demand-driven cross-price dependencies determine the impact of producer prices on the CPI inflation rate.

E-mail: christian.glocker@wifo.ac.at, philipp.piribauer@wifo.ac.at

2023/1/W/0

© 2023 Österreichisches Institut für Wirtschaftsforschung

Medieninhaber (Verleger), Hersteller: Österreichisches Institut für Wirtschaftsforschung

1030 Wien, Arsenal, Objekt 20 | Tel. (43 1) 798 26 01-0 | <https://www.wifo.ac.at>

Verlags- und Herstellungsort: Wien

WIFO Working Papers are not peer reviewed and are not necessarily based on a coordinated position of WIFO. The authors were informed about the Guidelines for Good Scientific Practice of the Austrian Agency for Research Integrity (ÖAWI), in particular with regard to the documentation of all elements necessary for the replicability of the results.

Kostenloser Download: <https://www.wifo.ac.at/wwa/pubid/70976>

PROPAGATION OF PRICE SHOCKS TO CPI INFLATION: THE ROLE OF CROSS-DEMAND DEPENDENCIES

CHRISTIAN GLOCKER AND PHILIPP PIRIBAUER

ABSTRACT. Cross-demand creates links between goods which cause demand-driven cross-price dependencies. We construct a theoretical model to analyze their role in propagating microeconomic price shocks to the CPI inflation rate and examine their empirical relevance using spatial econometric techniques. The results highlight the importance of complementarity and substitution properties between goods in exacerbating or mitigating price shocks. This contrasts with the propagation through the production network. Most importantly, demand-driven cross-price dependencies determine the impact of producer prices on the CPI inflation rate.

JEL codes: C11; C53; D85; E31

Key words: Inflation; Consumer behavior; Cross price dependencies; Network analysis

C. Glocker: Austrian Institute of Economic Research, Arsenal Objekt 20, 1030 Vienna, Austria. Phone: +43 (0) 1 789 26 01-303, E-mail: christian.glocker@wifo.ac.at

P. Piribauer: Austrian Institute of Economic Research, Arsenal Objekt 20, 1030 Vienna, Austria. Phone: +43 (0) 1 789 26 01-494, E-mail: philipp.piribauer@wifo.ac.at

This version: July 2023

The authors would like to thank Maximilian Böck, Serguei Kaniovski, Silvio Petriconi, Philipp Schmidt-Dengler, Nawid Siassi, Pascal Towbin, Thomas Url and Edgar Vogel for valuable comments and helpful discussions. Excellent research assistance by Astrid Czaloun is gratefully acknowledged.

1. INTRODUCTION

We analyze the role of microeconomic price shocks in shaping fluctuations in aggregate price measures such as the consumer price index (CPI). Our focus is on the links between prices and whether they can act as a channel for the propagation and amplification of shocks. Links between prices can arise for several reasons. First, from a (firm) supply side view, distinct goods (and services) may contain the same intermediate goods, resulting in cross-price dependencies that reflect value chains along production networks. Second, from a (consumer) demand side view, individual goods' price shocks may spill over to other goods' prices due to the complementarity or substitutability of goods.¹ Acemoglu et al. (2012) construct a theoretical model of a production network in which links between prices emerge from intra-industry relationships. In this setting, any additional link exacerbates microeconomic shocks. However, this is unlikely to be the case when considering the consumer demand side view, since the effect of an additional link depends on whether it arises from a complementary or substitutive relationship between goods. Consequently, microeconomic price shocks could either be exacerbated or mitigated.

Our contribution is threefold. First, we establish a theoretical model to capture the role of demand-driven links between prices for the CPI inflation rate. This serves to highlight that microeconomic price shocks diffuse through the demand system and hence may not remain confined to where they originate. Second, we estimate these links for a large set of countries and compare them to those from the supply side. This allows us to compare the size and sign of the spillover effects of microeconomic price shocks from demand- and supply-driven cross-price dependencies. Third, we examine the role of the structure of the demand-driven cross-price dependencies for the CPI inflation rate. This serves to empirically assess their role in the propagation and amplification of microeconomic price shocks to the CPI inflation rate through the demand system.

Assessing the transmission of microeconomic price shocks to a headline measure of inflation is currently an active area of research. However, the focus in this context has so far been limited to the supply side. Bilgin and Yılmaz (2018) consider a production network to examine how shocks to prices, rather than quantities, are transmitted across industries. They show that the input-output (I-O) linkages across industries form a network through which the price shocks are transmitted. Moreover, they cannot reject

¹For example, a high demand for restaurant visits (“catering services”) might not only raise prices in this subcomponent, but also in those which are closely related (“food”, “beverages”, “transport services”, etc.).

the hypothesis that their system-wide measure of the underlying network Granger-causes the system-wide measure of inflation linkages. As an extension, Bilgin (2022) shows how the underlying I-O linkages are responsible for the transmission of inflation. A common feature of these studies is their focus on the supply side. While it is clear that the effect of microeconomic price shocks can be amplified as they propagate through the production network, the same shocks can also propagate through the demand side. The extent of shock diffusion, in turn, shapes the overall inflation dynamics.

We therefore employ a simple theoretical general equilibrium model in which links between prices emerge from consumers' cross-demand, hence reflecting consumer preferences. Cross-demand captures the extent to which goods are related from a demand side view. This in turn creates links between the prices of goods which we will henceforth refer to as demand-driven cross-price dependencies. As cross-demands lead to complements or substitutes, the corresponding links between prices can be assigned negative or positive values. The model serves to examine the consequence of the demand-driven cross-price dependencies for shaping the spillover effects of microeconomic price shocks on the CPI inflation rate. The spillover effects reflect the degree of connectedness of the network of cross-price dependencies which can be decomposed into (i) a *strength* effect and (ii) a *diffusion* effect. While the former is determined by the size and sign of the links (edges) between prices (nodes), the latter is determined by the structure of the demand-driven cross-price dependencies. We use distinct network topology measures to capture the spillover effects arising from the strength and diffusion effect. We then estimate the key equation of the theoretical model to examine the empirical evidence for demand-driven cross-price dependencies. We apply a Bayesian spatial econometric framework and use the three-digit price subindices of the CPI for 28 countries (UK and the current EU member states) to compare the resulting links between prices with those emerging from a production network. The latter is based on the I-O tables which are converted into the CPI's Classification of Individual Consumption by Purpose (COICOP) using the concordance matrices of Cai and Vandyck (2020). Finally, the estimated price network is used to examine the first-order and second-order effects of the demand-driven cross-price dependencies (proxied by the network topology measures) on the CPI inflation rate.

Our contribution builds on two relatively recent developments. First, by drawing on tools from a diverse body of knowledge, the burgeoning field of graph theory has developed a conceptual framework and a comprehensive set of tools for effectively encoding and measuring the interconnections among the units of analysis that make up

a network. It serves as a tool for assessing how shocks propagate and how aggregate fluctuations can be traced back to localized micro-disturbances. Second, developments in econometric theory have established a set of models and theoretical instruments of spatial statistics and spatial data analysis to analyze various economic effects such as externalities, interactions and spatial concentration. These allow for efficient estimation of linkages across a large number of individual units.

To preview some results, we find empirical support for the existence of demand-driven cross-price dependencies which render the overall effect of microeconomic price shocks on the CPI inflation rate distinct to their mere direct effect. Most importantly in the context of consumer demand, the presence of substitutes and complements leads to an exacerbation or mitigation of microeconomic price shocks. In particular, we find, first, that positive valued links dominate which highlights the relative importance of the complementarity property among goods. Second, spillover effects of the price subindices on the CPI inflation rate are both negative and positive and their quantitative size outweighs the direct effects in most of the cases. The latter emerges from the high number of cycles among prices. Third, demand-driven links among prices show remarkable differences to a supply side counterpart and they tend to change over time, reflecting changes in consumer preferences. Most importantly, we find that the demand-driven cross-price dependencies explain a major part of the CPI inflation rate. We do so by proxying the corresponding spillover effects with distinct network topology measures and regressing them on the CPI inflation rate. We find that, while they explain significant variation in the CPI inflation rate by themselves, they critically shape the effects of other variables (e.g., producer prices, PPI) on the CPI inflation rate. This empirical result is consistent with the theoretical model and highlights the importance of the demand system for the diffusion of microeconomic price shocks to the CPI inflation rate.

Related literature. Our contribution is related to various strands of the literature. There is a long research on cross-price demand effects with a focus both on individual goods' prices and on composite price indices. Work by Mulhern and Leone (1991); Regmi and Seale (2010); Mehta and Ma (2012) highlight the dominance of substitutes, while others (van Oest, 2005) emphasize complements. Using 7,264 estimates from 115 studies, Auer and Papies (2020) find that the mean cross-price demand elasticity is 0.26 (median: 0.10), with high-stockpiling groceries having the highest cross-price elasticities. With a view to the composite price indices for goods categories, Regmi and

Seale (2010) highlight that among their nine categories of goods,² non-zero cross-price dependencies hold in 97 percent of all possible combinations. This finding applies to high, middle and low income countries, and the sign of the cross-price demand effects gives rise to a dominance of complements (67%). Hence, while price indices may appear independent to each other by virtue of their category's name, depending on which level of disaggregation one chooses, it is apparent that changes in one price (sub) index may have an impact on others. This is likely to be particularly relevant for the CPI, which constitutes a composite index that partitions all consumer goods and services into a hierarchy of increasingly detailed subindices. This establishes a connection with another important part of the literature concerning production networks. Acemoglu et al. (2012) construct theoretical models in which each industry depends on the output of other sectors, while combining these outputs as their intermediate inputs for production. Bilgin and Yilmaz (2018) and Bilgin (2022) extend these models to examine how producer prices diffuse through the I-O linkages in a multi-sector setting. Their empirical results highlight the importance of supply-driven cross-price dependencies for the inflation transmission. Afrouzi and Bhattarai (2022) extend this static setting to a dynamic one and show that in response to monetary policy and supply shocks, I-O linkages significantly increase the persistence of the CPI inflation rate relative to an economy with a horizontal production network.

In a similar context, several papers investigate the I-O linkages for inflation synchronization – including Di Giovanni and Levchenko (2010); Auer and Sauré (2013); Auer et al. (2019) – and report that countries that trade with each other exhibit higher inflation synchronization. Auer and Mehrotra (2014) examine cross-border price spillover effects in the Asian manufacturing supply-chain based on the World I-O database. Neely and Rapach (2011) characterize links in international inflation and find that the global component accounts for 35 percent of domestic inflation volatility. Ahmad and Staveley-O'Carroll (2017) highlight the structure of international price contracts that explain most of the differences in inflation volatility and persistence. Auer et al. (2019) document that international I-O linkages contribute substantially to the synchronization of producer price inflation (PPI) across countries, and that these linkages account for half of the global component of PPI inflation.

In a more general context, our contribution is also related to studies that examine the cross-country differences in inflationary dynamics. Hall et al. (2023) and Choi et

²The nine goods categories are: food, beverage and tobacco; clothing and footwear; gross rent, fuel and power; house operations; medical care; education; transport and communication; recreation; other items.

al. (2018) are recent contributions among others in this context, of which the former analyze commonalities in inflation dynamics across the US, the euro area and the UK, while the latter focus on the role of the oil price for a large panel of advanced and developing economies.

The paper is structured as follows. Section 2 presents the theoretical model and introduces the network topology measures to capture the spillover effects that emanate from the demand-driven cross-price dependencies. Section 3 motivates the econometric model to estimate the demand-driven cross-price dependencies and compares the resulting spillover effects with those from a supply side set-up. Section 4 extends the analysis by examining as to whether the structure of the cross-price dependencies matters for explaining the variation of the inflation rate. Finally, Section 5 concludes.

2. CONSUMER PREFERENCES AND INFLATION DYNAMICS

The purpose of this section is to illustrate the role of cross-price effects for inflation dynamics. We analyze cross-price effects as a result of consumer behavior and hence of preferences captured in the associated consumer demand functions. In this context, cross-price effects emerge due to the substitutability or complementarity of goods. We show how this matters for the impact of microeconomic price shocks on the CPI inflation rate.

2.1. Cross-price effects and the inflation rate. Consider a static economy with $n \in \mathbb{N}$ goods produced by a unit mass of firms. The total quantity of each of the n goods produced is given by $x_i^s \geq 0 \forall i = 1, \dots, n$, which in turn are supplied in perfectly competitive markets at market prices $p_i \in \mathbb{R} \forall i = 1, \dots, n$. We take a short term view and assume that the supply of each good x_i^s is perfectly inelastic with respect to its price p_i . Consumers in turn buy these goods. We consider a unit mass of representative consumers out of which consumer j 's consumption of the n different types of goods is given by the Walrasian (Marshallian) demand function $x_i^{j,d} = x_i^{j,d}(p_i, \mathbf{p}_{-i}, m^j) \forall i = 1, \dots, n$, with x_i^j being the quantity demanded of good i , m^j denotes the consumer's available budget and $\mathbf{p}_{-i} = [p_k]_{k=1}^{n \setminus \{i\}} \in \mathbb{R}^{n-1}$ is a vector of prices excluding the price of good i . Summation over the mass of consumers establishes the total demand for good i which is given by the total demand function $x_i^d = \sum_j x_i^{j,d} = x_i^d(p_i, \mathbf{p}_{-i}, \sum_j m_j)$, where the last step follows from the assumption of representative consumers. In equilibrium $x_i^s = x_i^d = x_i$, which gives rise to the following equilibrium quantity

$$(1) \quad x_i = x_i(p_i, \mathbf{p}_{-i}, m)$$

where $m = \sum_j m_j$ is consumers' total income. With the assumption of a perfectly price-inelastic supply, equilibrium prices are shaped by demand shocks only. This implies that, whenever a demand shock occurs, the equilibrium quantity x_i will be left unchanged and only the price p_i will be affected. The latter though, is likely to shape the demand for yet other goods $x_j \forall j \neq i$, which emerges from the circumstance that goods may be substitutes or complements to each other. This, in turn, will then also shape the prices of these goods ($p_j \forall j \neq i$), which establishes links across prices in equilibrium. In what follows, we use this set-up to elaborate on the role of cross-price dependencies for an aggregate price measure and its rate of change. It is useful to this purpose to express the demand function for good i as of equation (1) by means of its inverse demand function $p_i = p_i(x_i, \mathbf{p}_{-i})$. Collecting all goods' (inverse) total demand functions in the price vector function $\mathbf{p}^f(\cdot)$ gives the following vector of equilibrium prices

$$(2) \quad \mathbf{p}^f(\mathbf{p}, \mathbf{x}) = \begin{bmatrix} p_1(x_1, \mathbf{p}_{-1}) \\ \vdots \\ p_n(x_n, \mathbf{p}_{-n}) \end{bmatrix}$$

where all arguments beyond prices p_i are omitted in $p_i(\cdot)$ for simplicity. Letting $\mathbf{w} = [w_i]_{i=1}^n$ with $w_i \in [0, 1] \forall i = 1, \dots, n$ and $\sum_{i=1}^n w_i = 1$ be the vector of expenditure shares (that is, the weights) of the goods, then the consumer price index p (CPI), as an aggregate price measure, is given by $p = \mathbf{w}'\mathbf{p}^f(\mathbf{p}, \mathbf{x})$ and its change is

$$(3) \quad \Delta p = \mathbf{w}' \cdot \Delta \mathbf{p}^f(\mathbf{p}, \mathbf{x})$$

where $\mathbf{p} = [p_i]_{i=1}^n \in \mathbb{R}^n$ and the geometric mean, as used for constructing the CPI (IMF, 2022a), is approximated with the arithmetic mean. Observe that the price vector $\mathbf{p}^f(\mathbf{p}, \mathbf{x})$ is a function $\mathbf{p}^f: \mathbb{R}^n \rightarrow \mathbb{R}^n$ that takes a vector as input and produces a vector as output. We can identify the cross-price effects from this vector of inverse demand functions by the Jacobian matrix $\mathcal{A} = \nabla_{\mathbf{p}}\mathbf{p}^f(\mathbf{p}, \mathbf{x})$ which is a $n \times n$ matrix of partial derivatives and given by

$$(4) \quad \mathcal{A} = \begin{bmatrix} 0 & \dots & \frac{\partial p_1(x_1, \mathbf{p}_{-1})}{\partial p_n} \\ & \ddots & \\ \frac{\partial p_n(x_n, \mathbf{p}_{-n})}{\partial p_1} & \dots & 0 \end{bmatrix}$$

We will henceforth refer to \mathcal{A} as the *price-Jacobian* matrix. It tells us the relationship between changes in the input and changes in the output, for instance, considering the i, j element, the corresponding entry in \mathcal{A} identifies the effect of a change in p_j on p_i

which is given by $\Delta p_i = \frac{\partial p_i(x_i, \mathbf{p}_{-i})}{\partial p_j} \cdot \Delta p_j$. This can be generalized in matrix notation as $\Delta \mathbf{p}^f(\mathbf{p}, \mathbf{x}) = \mathcal{A} \cdot \Delta \mathbf{p}^f(\mathbf{p}, \mathbf{x})$. Adding to this relationship an exogenous demand shock in the form of a disturbance to the price of good i equal to \tilde{u}_i , then the own price effect is given by $\Delta p_i = \sum_{j=1}^n \alpha_{ij} \Delta p_j + \tilde{u}_i$ with $\partial p_i(x_i, \mathbf{p}_{-i}) / \partial p_j \equiv \alpha_{ij} \in \mathcal{A}$ and the effect on other goods' prices by $\Delta p_k = \sum_{j=1}^n \alpha_{kj} \Delta p_j \quad \forall k \neq i$. Since this relationship has to hold for all prices, it provides a system of equations to solve for all prices in terms of demand shocks. It can be rewritten in matrix form as

$$(5) \quad \Delta \mathbf{p}^f(\mathbf{p}, \mathbf{x}) = \mathcal{A} \cdot \Delta \mathbf{p}^f(\mathbf{p}, \mathbf{x}) + \tilde{\mathbf{u}}$$

where $\tilde{\mathbf{u}}$ is the vector of demand shocks $(\tilde{u}_1, \dots, \tilde{u}_n)$. Equation (5) solves for the change in the price vector as follows: $\Delta \mathbf{p}^f(\mathbf{p}, \mathbf{x}) = (I - \mathcal{A})^{-1} \tilde{\mathbf{u}}$, provided that the inverse of $I - \mathcal{A}$ exists (more on this in Section 2.2). From this equation we can then determine the effect on the CPI inflation rate by using equation (3), which implies

$$(6) \quad \pi = \mathbf{w}'(I - \mathcal{A})^{-1} \mathbf{u}$$

where the CPI inflation rate π is given by $\pi = \frac{\Delta p}{p}$ and $\mathbf{u} = \tilde{\mathbf{u}}/p$. As equation (6) illustrates, the CPI inflation rate is shaped by cross-price effects captured in the price-Jacobian matrix \mathcal{A} . If the price-Jacobian matrix is equal to the null matrix, then we have that $\partial \pi / \partial u_i = w_i$, which implies that the effect of a shock to an individual price on the CPI inflation rate equals this price's weight w_i times the size of the shock. When cross-price dependencies are present, the price-Jacobian matrix is then distinct to the null matrix and a shock to an individual price may affect the CPI inflation rate not only directly, but also via spillover effects arising from the cross-price dependencies. What matters in this context are (i) the sign of the off-diagonal elements in the price-Jacobian matrix \mathcal{A} reflecting the substitution and complementarity relationships among goods, and (ii) the structure that emerges from the cross-price dependencies. In what follows, we discuss this in more detail using graph theory.

2.2. On the price-Jacobian matrix. The price-Jacobian matrix \mathcal{A} in equation (5) is derived under the assumption of inelastic supply. It therefore only captures price effects of demand shocks. We establish equivalent relations to equations (5) and (6) from a supply side approach in Appendix A. It is useful to take a closer look at the properties of the price-Jacobian matrix \mathcal{A} and the matrix $\mathcal{L} = (I - \mathcal{A})^{-1}$. In the context of a production network the latter is commonly referred to as the economy's Leontief inverse (see Appendix A). There economic theory imposes certain restrictions on $(I - \mathcal{A})$

which guarantee the invertibility of \mathcal{L} and its representation as an infinite sum. While this does not apply in our case, several aspects are still worth to be highlighted.

First of all, the elements $\alpha_{ij} \in \mathcal{A}$ can have both positive and negative entries. This results from the substitution and complementarity of the goods. Consider goods i and j and their prices: a demand shock, for instance, in the form of a change in income m by dm , gives rise to $dx_i = 0 \ \forall i = 1, \dots, n$ due to the assumption on supply and hence only prices will react: $dp_i/dm = -\frac{dx_i/dm}{dx_i/dp_i} \ \forall i = 1, \dots, n$. Since $dp_i/dp_j = \frac{dp_i/dm}{dp_j/dm}$, we obtain the following expression for the cross-price dependencies by means of the total differential of equation (1)

$$(7) \quad \frac{\partial p_j}{\partial p_i} = \frac{dx_j/dp_i}{dx_j/dp_j} \begin{matrix} \leq 0 \\ > 0 \end{matrix}$$

Ruling out Giffen goods implies that $dx_j/dp_j < 0 \ \forall j = 1, \dots, n$. With regard to cross-price effects, whenever good i and j are complements ($dx_j/dp_i < 0$), we have that $\frac{\partial p_j}{\partial p_i} > 0$. Conversely, $\frac{\partial p_j}{\partial p_i} < 0$ when they are substitutes. In other words, the demand shock (dm) leads to a positive co-movement among prices of those goods that are complements, while the opposite applies to prices of goods that are substitutes.

Second, $\alpha_{ij} \neq \alpha_{ji}$ since in general $\frac{dx_i}{dp_j} \neq \frac{dx_j}{dp_i}$. Sethuraman et al. (1999) put forth two effects that matter from an empirical point of view in this context: the asymmetric price effect and the neighborhood price effect. The asymmetric price effect states that cross-price elasticities are larger when the price changing good has a higher price than the demand changing good. Under the neighborhood price effect, cross-price elasticities are larger when the two competing goods are closer in price.

Third, the price-Jacobian matrix \mathcal{A} captures both own- and cross-price elasticities. Defining by $\varepsilon_i = \frac{dx_i/x_i}{dp_i/p_i}$ the (uncompensated) own-price elasticity and by $\varepsilon_{ij} = \frac{dx_i/x_i}{dp_j/p_j}$ the cross-price elasticity of demand, the elements α_{ij} are given by $\alpha_{ij} = \frac{\varepsilon_{ij}}{\varepsilon_i} \frac{p_i}{p_j}$, and the price-Jacobian matrix can then be decomposed in the following form

$$(8) \quad \mathcal{A} = -\mathbf{E}^{-1} \cdot \mathbf{H}$$

where $\mathbf{E} = \text{diag}(|\varepsilon_1|, \dots, |\varepsilon_n|)$ and $\mathbf{H} = [\eta_{ij}]_{i,j=1}^n$ with $\eta_{ij} = \varepsilon_{ij} \frac{p_i}{p_j} \begin{matrix} \leq 0 \\ > 0 \end{matrix} \ \forall i \neq j$ and $\eta_{ij} = 0 \ \forall i = j$. The matrix \mathbf{E} captures the own-price effects while \mathbf{H} the cross-price demand effects. In what follows, we assume that $\sum_{j=1}^n \varepsilon_{ij} \frac{p_i}{p_j} < |\varepsilon_i| \ \forall i = 1, \dots, n$. Under this assumption, all column-sums of the price-Jacobian matrix \mathcal{A} are less than unity. This motivates the following Lemma.

Lemma 1. *If $\sum_{j=1}^n \varepsilon_{ij} \frac{p_i}{p_j} < |\varepsilon_i| \forall i = 1, \dots, n$, then the matrix \mathcal{L} can be expressed as an infinite sum of the price-Jacobian matrix \mathcal{A} , that is*

$$(9) \quad \mathcal{L} = (I - \mathcal{A})^{-1} = \sum_{k=0}^{\infty} \mathcal{A}^k$$

The proof of Lemma 1 follows directly from the relation between any matrix norm and the spectral radius.³ Important for our context, Lemma 1 illustrates that the (i, j) element of the matrix \mathcal{L} captures the importance of price j as a direct and indirect shock transmitter to price i . To see this, note that, for any $i \neq j$, Lemma 1 implies that $l_{ij} = \alpha_{ij} + \sum_{h=1}^n \alpha_{ih} \alpha_{hj} + [\dots]$, with the first term in this expression accounting for price j 's role as a direct shock transmitter to price i , the second term accounting for price j 's role as a transmitter to the recipients of price i , and so on. Interpreted in terms of a network, l_{ij} accounts for all possible directed walks (of various lengths) that connect price j to price i over the network.

Fourth, in general, most non-zero entries in \mathcal{A} are likely to be small in amount. This follows from the fact that, on the one hand, mean cross-price elasticities are found to have small values in amount in most situations⁴ and, on the other hand, cross-price elasticities enter $\alpha_{ij} \in \mathcal{A}$ only relative to a good's own price elasticity, which is likely to be larger in amount.

2.3. The price-Jacobian matrix as a Graph. The price-Jacobian matrix \mathcal{A} can be considered as a directed weighted graph $\mathcal{G} = (\mathcal{N}, \mathcal{E}, \mathcal{A})$, where the $n > 1$ nodes in $\mathcal{N} = \{\nu_1, \dots, \nu_n\}$ represent the goods' prices $\Delta p_i \forall i = 1, \dots, n$, which are related to each other via the edges $\mathcal{E} \subseteq \mathcal{N} \times \mathcal{N}$, and the weight matrix $\mathcal{A} \in \mathbb{R}^{n \times n}$ determines the size (and sign) of the edges. Hence, the elements $\frac{\partial p_i(x_i, \mathbf{p}_{-i})}{\partial p_h} \forall i, h = 1, \dots, n$ with $i \neq h$ quantify the strength of the network's edges across nodes i and h , that is, $\nu_i \nu_h \in \mathcal{E} \iff \frac{\partial p_i(x_i, \mathbf{p}_{-i})}{\partial p_h} \neq 0$ with $\frac{\partial p_i(x_i, \mathbf{p}_{-i})}{\partial p_h} \in \mathcal{A}$.

In order to illustrate the role of the network structure for the effects of the cross-price dependencies on the CPI inflation rate, we assume that all non-zero edges have the same weight $\alpha_{ij} = \alpha$. We further simplify the exposition by considering a graph with three prices ($n = 3$), each represented by a node in the network (both assumptions are

³Werner (2009) shows that for any real matrix \mathcal{M} we have that $\rho(\mathcal{M}) \leq \|\mathcal{M}\|$, where $\|\cdot\|$ denotes any natural norm and $\rho(\mathcal{M})$ is the spectral radius which is defined as the maximum of the absolute values of the eigenvalues of \mathcal{M} . Then it follows that $\rho(\mathcal{M}) \leq \|\mathcal{M}\|_{\infty}$, the maximum absolute row sum, and $\rho(\mathcal{M}) \leq \|\mathcal{M}\|_1$, the maximum absolute column sum. So, if the row sum or the column sum of the matrix \mathcal{M} is less than unity, then these results verify the spectral radius condition. In this case, $I - \mathcal{A}$ is invertible and can be written as the Neumann-series $\sum_{k=0}^{\infty} \mathcal{A}^k = (I - \mathcal{A})^{-1}$.

⁴Auer and Papiés (2020) find an overall mean cross-price elasticity of 0.26 with 70 percent of all observations being below the mean, and a median of 0.10; similar values (in amount) are provided in Regmi and Seale (2010).

relaxed in the empirical part). The focus is explicitly on the network's structure in order to assess its consequence for the inflation rate π . To this purpose, we assume that each price has the same weight w in the CPI.

Table 1 shows several simple network structures (first column) and their consequences for the CPI inflation rate in response to a shock in the first price (u_1). We establish the adjacency matrix \mathcal{A} for the five cases, (a)–(e), and compute the CPI inflation rate π using equation (6). In the absence of links, the effect of a shock to the first price by $u_1 = 1$ on the CPI inflation rate equals $\pi^{(a)} = w$ (the superscript “(a)” refers to the case considered). Hence the effect of the shock (u_1) on the CPI inflation rate equals the weight w of the first price times the size of the shock. The introduction of links between the prices changes the effect of the shock on the CPI inflation rate. This is documented algebraically in the second column. The presence of links leads to spillover effects (ς) given by

$$(10) \quad \varsigma = \mathbf{w}' \left((I - \mathcal{A})^{-1} - I \right) \mathbf{u}$$

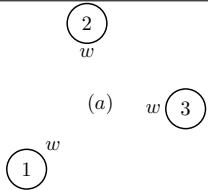
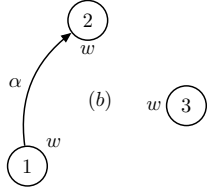
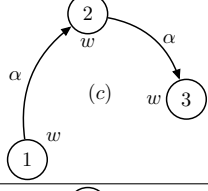
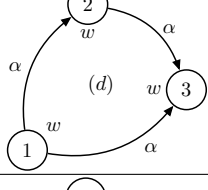
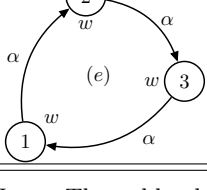
that is, the effects relative to those emanating from the zero-link case (a): $\varsigma^{(i)} = \pi^{(i)} - \pi^{(a)}$. Importantly, the spillover effects emerge from the cross-price dependencies and they reflect the degree of connectedness in the network. The degree of connectedness is in turn shaped by (i) a *strength* effect and (ii) a *diffusion* effect. When no links are present, the price-Jacobian matrix is equal to the null matrix. Hence, the spillover effects are equal to zero as neither a strength nor a diffusion effect applies. When the goods are complements to each other ($\alpha > 0$), then the strength effect implies that the degree of connectedness (and hence the spillover effects) increases with α , as can be seen in case (b): $\partial \varsigma^{(b)} / \partial \alpha = w > 0$. Conversely, the diffusion effect implies that the degree of connectedness (and hence the spillover effects) is determined by the number of links ($\varsigma^{(b)} < \varsigma^{(e)} < \varsigma^{(d)}$) and by the structure of the links in directed networks⁵ (acyclic or cyclic network structures: $\varsigma^{(d)} < \varsigma^{(e)}$ when $\alpha \in (0, 1)$).

A complication arises from the fact that goods may be substitutes to each other ($\alpha < 0$). Considering case (c), we then have that $\partial \varsigma^{(c)} / \partial \alpha = w + 2w\alpha \gtrless 0$, which implies that for certain network structures, the strength (and diffusion) effect can go either way.

The network structure is typically captured by so called network topology measures. The challenge in this respect is to establish network topology measures that adequately capture the variation in the spillover effects due to distinct network structures and edge

⁵More precisely, the network in case (d) constitutes an *acyclic* graph (commonly referred to as *directed acyclic graph*, DAG) and the network in case (e) is a *cyclic* graph.

TABLE 1. Examples of network structures

Network topology (cases)	Spillover effect of shock $u_1 = 1$	Link density	Network density	Graph energy
 <p>(a)</p>	$\zeta^{(a)} = 0$	0	0	0
 <p>(b)</p>	$\zeta^{(b)} = w\alpha$	$\frac{1}{3}$	$\frac{\alpha}{3}$	0
 <p>(c)</p>	$\zeta^{(c)} = \zeta^{(b)} + w\alpha^2 = w\alpha(1 + \alpha)$	$\frac{2}{3}$	$\frac{2\alpha}{3}$	0
 <p>(d)</p>	$\zeta^{(d)} = \zeta^{(c)} + w\alpha = w\alpha(2 + \alpha)$	1	α	0
 <p>(e)</p>	$\zeta^{(e)} = \frac{w\alpha}{1-\alpha}$	1	α	$2 \alpha $

Note: The table shows distinct network structures and their implications for the spillover effects ζ from a shock to the first price by $u_1 = 1$. The table also displays the values of three distinct network topology measures—link density (LD), network density (ND) and graph energy ($GE_{\mathbb{R}}$)—for each network structure. For $\alpha = 1$, we have that $GE_{\mathbb{R}} = GE_{\mathbb{Z}_2}$.

weights α . In what follows, we introduce three distinct network topology measures to capture the spillover effects.

2.4. Network topology measures and spillover effects. We use network topology measures to capture the size and the sign of the spillover effects, paying attention to strength and diffusion effect. The former concerns the quantitative size of the link between two connected nodes, while the latter concerns the amount of links and the overall arrangement of the links. We consider the following network topology measures:

- (1) Link density (LD): This measures how many links exist between nodes relative to the maximum possible number of links (Newman, 2010). Link density is thus a measure for the diffusion effect. For a graph with an $N \times N$ adjacency matrix $B = [\beta_{ij}]_{i,j=1,\dots,N}$ with $B \neq B'$, the link density is given by the scalar

$LD(B) = \frac{\sum_i^N \sum_{j \neq i}^N \mathbb{1}_{\{|\beta_{ij}| > 0\}}}{N(N-1)} \in [0, 1]$ where N is the number of nodes and $\mathbb{1}_{\{|\beta_{ij}| > 0\}}$ is the indicator function, which takes on a value of one if the condition $|\beta_{ij}| > 0$ is satisfied. The link density measures the diffusion effect.

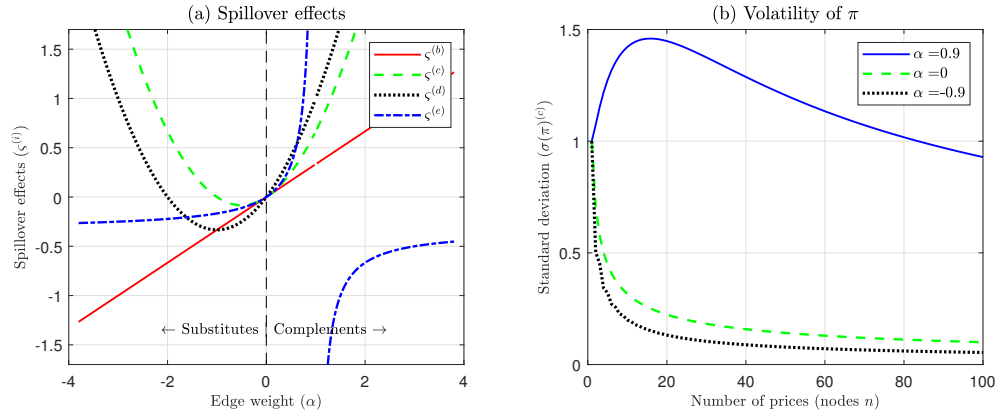
- (2) Network density (ND): For the same graph as before, the network density (Horvath, 2011) is given by the scalar $ND(B) = \frac{\sum_i^N \sum_{j \neq i}^N \beta_{ij}}{N(N-1)} \in \mathbb{R}$. It extends the link density by taking into account the weight of each edge $\beta_{ij} \in B$. Thus, for a given link density, the network density measures the strength effect.
- (3) Graph energy (GE): For the same graph as before, the graph energy is defined by the scalar $GE(B) = \sum_{i=1}^N |\Re(z_i)|$, where $\Re(z_i)$ is the real part of the complex number z_i , and the $z_i \forall i = 1, \dots, N$ are the eigenvalues of the adjacency matrix B . (Gutman, 1978; Peña and Rada, 2008). $GE(B) = 0$ means that a network has a perfect tree-like structure in which no loop is formed. Thus, the higher the graph energy,⁶ the more cyclic is the architecture of the network. We consider two versions of graph energy: the first is given by $GE_{\mathbb{Z}_2} \geq 0$ (henceforth binary GE) and is based on $\beta_{ij} \in B$ with $\beta_{ij} \in \{0, 1\} \forall i, j = 1, \dots, N$ and $i \neq j$ and the second by $GE_{\mathbb{R}} \geq 0$ (henceforth non-binary GE) which is based on $\beta_{ij} \in B$ with $\beta_{ij} \in \mathbb{R} \forall i, j = 1, \dots, N$ and $i \neq j$. The first measure ($GE_{\mathbb{Z}_2}$) captures the diffusion effect solely, while the second ($GE_{\mathbb{R}}$) captures both the diffusion and the strength effect.

We show the values of the three network topology measures for each of the five cases (a)–(e) in the third to fifth columns of Table 1. Their adequacy for our analysis is determined by their ability to capture the size and sign of the spillover effects.

Considering Table 1, in the absence of links, no spillover effects arise ($\zeta^{(a)} = 0$) and the three topology measures (LD, ND, and GE) are all equal to zero. When links are present, spillover effects occur. Whenever the goods are complements ($\alpha > 0$), increasing the number of links leads to yet larger spillover effects (second column) due to the diffusion effect. This is captured by the link density (third column) and applies to the cases (b)–(d). However, for the same cases, the presence of substitutes ($\alpha < 0$) renders the spillover effects negative, thus mitigating the effects of the shock. While the link density fails to capture this, the network density in turn does (fourth column), as it captures the strength effect, which in turn is affected by the sign of the edges. Importantly, though, a positive spillover effect can also occur in the case of substitutes.

⁶There are various alternatives, as for instance, the *R-measure* of Kim and Kim (2005). They propose a cyclic coefficient R that represents the cyclic characteristics of complex networks (R : cycle coefficient). Another interesting network topology measure in this context is given by the *cycle ratio* as proposed by Fan et al. (2021), or the cycle nodes ratio (CNR), which describes the ratio of the number of nodes belonging to cycles to the number of total nodes (Zhang et al., 2021).

FIGURE 1. Spillover effects and inflation



Note: Panel (a) shows the spillover effects of a unit-shock to the first node ($u_1 = 1$) for varying values of the edge weight α for a given node weight $w = 1/3$. Panel (b) shows the volatility of the CPI inflation rate as a function of the number of prices (nodes, n) in the network (each price i has a weight $w_i = 1/n$ in the CPI) for three distinct values of the edge weight α .

This is indicated by cases (c) and (d) and is shown in Figure 1, which illustrates the spillover effects for varying edge weights α .

Finally, case (e) comprises an interesting alternative network structure. It shares similarities with cases (c) and (d). The similarity with case (c) emerges from the fact that the CPI inflation rate for the network structure in case (c) is given by

$$(11) \quad \pi^{(c)} = \frac{w}{1 - \alpha}$$

and the spillover effect by $\zeta^{(c)} = \frac{w\alpha}{1 - \alpha}$ once the number of nodes n becomes large and each node (except the first and the last) has exactly one in-degree and one out-degree,⁷ and $|\alpha| < 1$. In this case, the two networks have the same spillover effects despite their distinct structures. In contrast, as regards cases (d) and (e), while the link and network densities are the same for these two cases, the graph energy is not. In particular, the spillover effect arising from case (e) can indeed be sizeable, especially in the case of complements⁸ (see Figure 1). Hence, the link and network density fail to capture this effect adequately from a quantitative point of view. Importantly, the effect emerges from a cyclical feature: Cases (b)–(d) represent *acyclic* networks, each with a nilpotent adjacency matrix. Case (e), on the other hand, is a *cyclic* network, which differs from the previous ones in that once a shock hits this network, a series of knock-on effects arise from the fact that the shock is continuously transmitted through the nodes forming the cycle (Boccaletti et al., 2006). From a technical point of view, the adjacency matrix

⁷In particular, the network is given by: (Node 1) \rightsquigarrow (Node 2) \rightsquigarrow (...) \rightsquigarrow (Node n). In this case, $\zeta^{(c)} = w\alpha \sum_{i=0}^{n-1} \alpha^i = \frac{w\alpha}{1 - \alpha}$ if $|\alpha| < 1$, which is the same as in case (e).

⁸If the cycle involves only two nodes: (Node 1) \rightsquigarrow (Node 2), then $\pi = \frac{w}{1 - \alpha}$ and $\zeta = \frac{w\alpha}{1 - \alpha}$, which is the same as in case (e), where the cycle involves three nodes.

has non-zero eigenvalues (Newman, 2010). While the number of non-zero eigenvalues depends on the number of cycles present in the network, we hence use an overall eigenvalue measure, which is given by the graph energy.⁹ This measure captures spillover effects emerging from cycles.

2.5. Individual price shocks and inflation dynamics. While the previous section illustrated the extent to which cross-price dependencies can act as a mechanism for propagating shocks from one good's price to the CPI inflation rate, we now examine whether they play a role for the inflation volatility.

Using equation (6) and setting the price-Jacobian matrix \mathcal{A} equal to the null matrix (case (a) of Table 1) implies that the volatility of the CPI inflation rate π that is due to idiosyncratic microeconomic price shocks is given by

$$(12) \quad \sigma(\pi)^{(a)} = \|\mathbf{w}\|$$

where $\sigma(\cdot)$ denotes the standard deviation and the demand shocks' variance is given by $E[\mathbf{u}\mathbf{u}'] = I$. Since $\|\mathbf{w}\| = (\sum_{i=1}^n w_i^2)^{1/2}$, equation (12) highlights that more dispersion in the weights \mathbf{w} can result in higher levels of volatility emerging from purely idiosyncratic shocks. In this regards, Gelos and Ustyugova (2017) highlight that countries with a higher weight of food in the CPI experience more persistent inflationary effects from commodity price shocks. In the absence of dispersion in the weights ($w_i = w \forall i = 1, \dots, n$), we have that

$$(13) \quad \sigma(\pi)^{(a)} = \frac{1}{\sqrt{n}}$$

since the weights \mathbf{w} satisfy $\sum_{i=1}^n w_i = 1 = nw$. This equation implies that when the weights of all prices are identical, the volatility of the inflation rate is proportional to $1/\sqrt{n}$, which is consistent with the diversification argument put forth in the context of production networks (Acemoglu et al., 2012; Fadinger et al., 2022) and financial networks (Tetryatnikova, 2014; Glasserman and Young, 2016; Das et al., 2022; Balcilar et al., 2023). However, the presence of cross-price dependencies can render the effects of a shock from any individual price large, irrespective of the dispersion of the weights. In this case, the prices of goods would be correlated, and thus individual price shocks may not disappear when aggregated, even if the shocks themselves are independent. Consider case (c) of Table 1, where $|\alpha| < 1$ and n is large; the effect of a shock to u_1 on the CPI inflation rate is given in equation (11); generalizing this result to the vector of

⁹With a view to Table 1, for $\alpha = 1$ we have that $\text{GE}_{\mathbb{R}} = \text{GE}_{\mathbb{Z}_2}$.

shocks \mathbf{u} , we then obtain the following

$$(14) \quad \sigma(\pi)^{(c)} = \frac{1}{(1-\alpha)\sqrt{n}}$$

which implies that $\sigma(\pi)^{(c)} > \sigma(\pi)^{(a)}$ whenever $\alpha > 0$ due to network spillover effects. The above equation highlights that there is a trade-off between the network and the volatility of the CPI inflation rate: A higher degree of connectedness—either via the strength effect (higher value of $|\alpha|$) and/or the diffusion effect (larger number of connections)—exacerbates the effect of microeconomic price shocks on the CPI inflation rate. The effect is attenuated by the degree of diversification, that is, a high n . This argument, however, only holds when cross-price dependencies emerge in the wake of complements ($\alpha > 0$), as illustrated in panel (b) of Figure 1. When dependencies arise from substitutes, then both the network effect (higher or lower degree of connectedness) and the diversification effect operate in the same direction rendering the mitigation of microeconomic shocks especially strong. In other words, each shock dissipates quickly and exerts an effect on the CPI inflation rate that is smaller than its pure direct effect.

3. ESTIMATING THE PRICE-JACOBIAN MATRIX

If the equilibrium conditions $x_i(p_i, \mathbf{p}_{-i}, m) \forall i = 1, \dots, n$ set out in Section 2.1 are based on homothetic consumer preferences¹⁰, then the rate at which a consumer is willing to substitute one good for another is independent of his income level. This, in turn, implies homogeneity of expenditure patterns across consumers with different income levels, that is, consumers spend the same share of their total expenditure on particular goods regardless of differences in income (Jehle and Reny, 2011). Since the assumption of homothetic preferences is at the core of the CPI (see Diewert, 2009; IMF, 2022b, among others), we estimate the price-Jacobian matrix \mathcal{A} by proxying the elements in the price vector of equation (2) by subcomponents of the CPI.

The goods and services in the CPI basket are classified by purpose into consumption groups (COICOP) at various levels of (dis-)aggregation, which are referred to as *structure levels* (two-digit, three-digit, etc.). We use the three digit COICOP structure of the CPI, which consists of 44 distinct monthly price subindices $P_{i,t}$. From these we exclude all those subindices for which the sample does not date back until (at least) 2004. This involves the price subindices related to educational goods and services (cp_101

¹⁰Homothetic preferences apply when the utility function $u(\mathbf{x})$ has a linear homogeneity property, which means that u satisfies the following condition: $u(\lambda\mathbf{x}) = \lambda u(\mathbf{x})$ for all $\lambda > 0$ and all $\mathbf{x} \in \mathbb{R}_+$. This assumption implies that each indifference curve is a radial projection of the unit utility indifference curve. It also implies that all income elasticities of demand are unity.

to cp_105), leaving a total of $n = 39$ subindices and their respective basket weights.¹¹ The details of the subindices are provided in Table 4 in the Appendix. We collect these data for 28 countries (the UK and the current EU member states).

Our choice of the three-digit COICOP level is motivated by our ambition to compare demand- with supply-driven cross-price dependencies for which we rely on the work of Cai and Vandyck (2020). They establish concordance matrices that map the statistical classification of the input-output (I-O) tables to the COICOP classification. These matrices are limited to the three-digit COICOP level, so we only consider the price subindices of this level of disaggregation. Most importantly, based on the model presented in the Appendix, a supply side version of the price-Jacobian matrix can be constructed and calibrated by using the I-O tables and the concordance matrices of Cai and Vandyck (2020). This then allows the cross-price dependencies of the supply side ($\tilde{\Gamma}$) to be directly compared with those of the demand side ($\tilde{\mathcal{A}}$).

3.1. The econometric methodology. We estimate the price-Jacobian matrix of equation (5) by relying on spatial econometric methods and consider the following empirical model to this purpose

$$(15) \quad \mathbf{y}_t = \mathbf{A}\mathbf{y}_t + \mathbf{X}_t\boldsymbol{\beta} + \boldsymbol{\varepsilon}_{yt},$$

where \mathbf{y}_t is a vector of length n of the dependent variables measured at time $t = 1, \dots, T$, \mathbf{X}_t is an $n \times Q$ matrix of control (or explanatory) variables with a corresponding slope parameter vector $\boldsymbol{\beta}$, where the matrix \mathbf{X}_t may also include fixed effects. $\boldsymbol{\varepsilon}_{yt}$ is an n -dimensional error term, and the $(n \times n)$ matrix \mathbf{A} governs the interaction between the cross-sectional observations (i.e. the n price subindices). The dependent variable comprises information on $n = 39$ price subindices (three-digit level of the CPI) and they enter the vector \mathbf{y}_t in annual percentage changes. The monthly data set starts in January 2000 and¹² ends in May 2022, which implies that $T = 269$. We estimate equation (15) individually for each country and rely on Bayesian methods for the statistical inference. We use an $n \times n$ matrix $\underline{\mathbf{A}}$, which comprises prior knowledge on \mathbf{A} , along with Dirichlet-Laplace shrinkage priors (Bhattacharya et al., 2015) to avoid over-parameterization. Our model set-up is thus a Bayesian Markov chain Monte-Carlo (MCMC) version, reminiscent of recent work by Gefang et al. (2022) and Lam and Souza (2020). We follow Lam and Souza (2020) for the estimation of \mathbf{A} and construct instruments from within the model by interacting the expert prior information $\underline{\mathbf{A}}$ with

¹¹The weights were re-adjusted to account for the omission of five subindices.

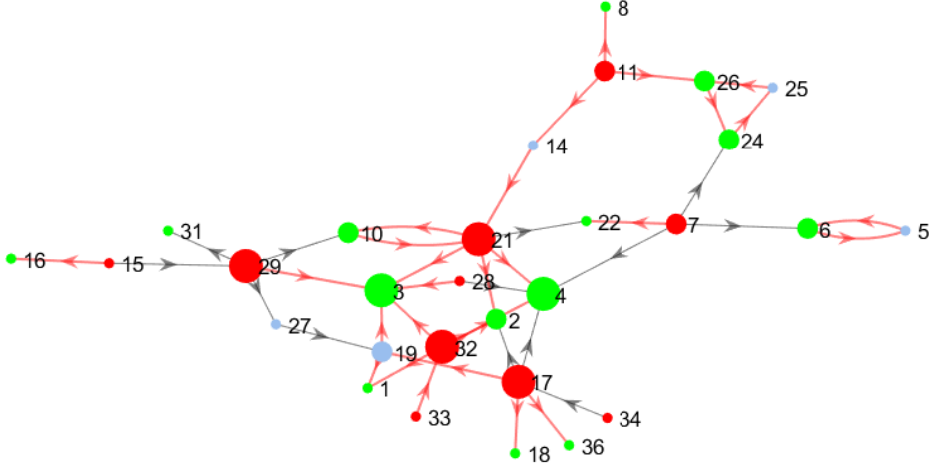
¹²For some countries, the sample of the CPI data starts later than January 2000. In these cases we use the earliest available data.

the exogenous variables. We rely on the estimates in Table 4 in Regmi and Seale (2010) as a prior information for \mathbf{A} and distinguish between high-income and low-income countries, and hierarchical shrinkage is applied to these estimates. Alternatively, no external prior information is used, the elements in \mathbf{A} are shrunk to a sparse matrix. For inference, we sample 1,000 MCMC draws for each country and discard 750 as burn-ins. Further technical details are provided in the Appendix.

The values of the vector $\boldsymbol{\beta}$ are interpreted as average immediate effects of changes in the explanatory variables on the dependent variables of the same price subindex (Asgharian et al., 2018; Karamysheva and Seregina, 2022). The matrix \mathbf{A} governs the interaction between the dependent variables (commonly referred to as the weighting matrix) and has zeros on its main diagonal and is not symmetric. The elements in this matrix indicate the relative closeness of the price subindices to each other. More specifically, the element in row i and column j of the matrix shows the reaction of the price subindex i to a change in the price subindex j . This element is therefore a measure of the cross-price effects of the price subindex i on changes in the price subindex j (Heil et al., 2022; Hall et al., 2022).

Our attempt to estimate demand-driven cross-price dependencies is based on the idea of estimating inverse demand functions. In this setting, however, the classic identification problem arises as prices are the result of the interplay between supply and demand. Thus, assuming that markets clear, prices are hence equilibrium outcomes. In principle, there is no endogeneity problem if supply is price inelastic (this could be relevant for administered prices and/or supply in the short run). In general, however, this is not the case. What is needed conceptually is a way to keep demand constant while varying supply. We therefore use a large set of supply side variables in the vector of explanatory variables (\mathbf{X}_t) that do not directly affect demand (but only indirectly through the price variable). Thus, after controlling for supply side influences, we can capture the demand-driven cross-price dependencies in the matrix \mathbf{A} . Our set of explanatory variables includes several price subindices of the producer price index (price indices for the manufacture of food products, beverages and tobacco products; for the manufacture of textiles, wearing apparel, leather and related products; for intermediate goods; for energy; for capital goods; for durable consumer goods; for non-durable consumer goods; and for mining and quarrying), a measure of administered prices, the nominal effective exchange rate and global measures such as shipping costs (Carrière-Swallow et al., 2023), the oil price (Brent) and a price measure for natural gas (Dutch TTF). In addition, we use the overall CPI inflation rate as a control variable. This is

FIGURE 2. Cross price dependencies



Note: The figure shows the cross-price dependencies as a network. We only show the edges that are present in 50 percent of the countries. Nodes in red indicate out-degree dominance, while those in green indicate in-degree dominance; nodes in blue indicate equality between out- and in-degree. Edges in red refer to positive valued links (complements, $\alpha_i > 0$) and those in black to negative ones (substitutes, $\alpha_i < 0$).

motivated by the common practice in many industries (insurance and telecommunication services, for instance) to adjust prices on the basis of the past CPI inflation rate (inflation indexation of prices). These variables are used for each country.

We transform the estimated matrix \mathbf{A} of equation (15) into an adjacency matrix $\tilde{\mathcal{A}}$ by applying the following statistical thresholding

$$(16) \quad \tilde{\alpha}_{ij} = \begin{cases} a_{ij} & \text{if } \forall i \neq j : \Pr(a_{ij} \neq 0) \geq 1 - \bar{p} \\ 0 & \text{else} \end{cases}$$

where $a_{ij} \in \mathbf{A}$ and $\tilde{\alpha}_{ij} \in \tilde{\mathcal{A}}$, and we use a significance value of p equal to one percent. These values define the edges of the weighted directed network of empirical cross-price dependencies. Since we have a posterior distribution for \mathbf{A} , the same then applies to the adjacency matrix $\tilde{\mathcal{A}}$ (in particular, its non-zero elements). We keep all those posterior draws of $\tilde{\mathcal{A}}$ that satisfy Lemma 1. On average (across countries), three percent of the draws are discarded as a consequence.

3.2. The empirical cross price dependencies. Figure 2 shows the empirical cross-price dependencies given by the matrix $\tilde{\mathcal{A}}$ across all countries. We display only those edges that are present in 50 percent of the countries, in order to allow for a reasonable inspection of the most relevant links. Edges in red refer to positive entries ($\alpha_{ij} > 0$, complements) and those in black to negative ones ($\alpha_{ij} < 0$, substitutes).

TABLE 2. Network topology statistics

	Demand side ($\tilde{\mathcal{A}}$)		Supply side ($\tilde{\Gamma}$)	
	Mean	Standard deviation	Mean	Standard deviation
Positive edges ratio ⁽¹⁾	0.76	0.03	1	0
Link (degree) density (LD)	0.26	0.07	0.33	0.09
Network density (ND)	0.01	0.01	0.15	0.00
Graph energy (non-binary, $GE_{\mathbb{R}}$)	2.01	0.54	9.64	1.56
Graph energy (binary, $GE_{\mathbb{Z}_2}$)	12.77	3.63	25.18	4.76
(Dis-) Assortativity ⁽²⁾	-0.06	0.06	-0.27	0.07
				Cosine-similarity
	Sensitivity	Specificity	Accuracy	
Similarity of $\tilde{\mathcal{A}}$ to $\tilde{\Gamma}$ ⁽³⁾	0.04	0.52	0.26	0.02
	(0.01)	(0.03)	(0.08)	(0.04)

Notes: The moments (*Mean* and *Standard deviation*) are computed for each network topology measure across the countries.

⁽¹⁾ *Positive edges ratio* denotes the number of edges with a positive value relative to the total number of non-zero edges.

⁽²⁾ Assortativity (Dis-assortativity if negative) is a measure of the preference of nodes in a network to attach to others that are (dis-)similar in terms of their degree. It is operationalized as the correlation between two nodes.

⁽³⁾ The figures shown are the mean and the standard deviation (in parenthesis) across the countries.

The estimated cross-price dependencies imply, for instance, that an increase in demand for food (node 1) leads to higher prices in this group and to price changes in two closely related groups, that is, non-alcoholic beverages (node 2) and tobacco (node 4), both of which are affected positively, creating complementary effects. Food prices are in turn shaped by the prices of catering services (node 32), which also affect the prices of alcoholic beverages (node 3).

As a second example, consider an increase in rental prices for housing (node 7), which triggers substitution effects for tobacco (node 4) and clothing (node 6). The latter in turn forms a cycle with footwear (node 5), that is, higher demand for clothing raises demand for footwear with price increases in both groups; higher demand for footwear in turn stimulates demand for clothing with another round of price increases in both groups. The interaction is shaped by positive-valued edges resulting in goods being complementary to each other. Table 2 highlights that the complementarity property of goods dominates. The mean (across countries) of the ratio of positive-valued edges to the total number of non-zero edges equals 76 percent, which is well in line with the 67 percent estimate in Regmi and Seale (2010). A cross-country mean value of 26 percent for the link (degree) density contrasts a fairly low value for network density due to negative-valued edges.

The cross-price dependencies as shown in Figure 2 emerge from demand dynamics as we control for a wide range of supply side factors in the estimation. This naturally raises the question as to what extent they differ to the supply side cross-price dependencies. We show the supply side driven cross-price dependencies in Figure 5 in the Appendix. They are based on a simple supply side model, which is a version of the model considered in Acemoglu et al. (2012). The model is calibrated using, among others, the I-O tables. Most importantly for our purposes, the statistical classification of the I-O tables was mapped to the COICOP classification by using the concordance matrices of Cai and Vandyck (2020). A direct visual comparison of the two networks of cross-price dependencies reveals notable differences, as do the network statistics provided in Table 2. First, the supply side network has a high level of dis-assortativity (negative degree correlation), but also a high extent of assortative hubs (nodes 1, 3, 10 and 39). Colizza et al. (2006) point out that most real-world (scale-free) networks have this feature. A closer look reveals that these hubs have a significant out-degree dominance. The implication for the network is that a small set of nodes shapes the network’s overall dynamics. In contrast to that, the demand-driven cross-price dependencies show a lower extent of dis-assortativity with a more balanced distribution of the nodes with out-degree dominance. Second, the supply-driven network displays a high clustering tendency, which is manifested in the form of nodes being divided into three blocks. The network aligns with a so called *stochastic block model* (Frank and Harary, 1982; Holland et al., 1983; Karrer and Newman, 2011). The implication is that the network’s dynamics are determined by the interaction of the nodes in these blocks, which in turn are shaped by the hubs in these blocks. Such block clustering is absent in the demand-driven network of cross-price dependencies. Third, both networks share a high degree of cyclicity. For instance, the demand-driven network has three individual cycles (nodes 5 and 6; nodes 10 and 21; nodes 24, 25 and 26) while the supply-driven network has two (nodes 1 and 3; nodes 7 and 39). In each case this gives rise to a high overall extent of network dynamics, as indicated by the high values of graph energy (see Table 2).

Although the previous analysis already indicated significant differences between the price dependencies of the demand side and the supply side, we now formalize this using statistical criteria. The accuracy of the estimated demand-driven price dependencies (and hence the quality of the estimation of the matrix \mathbf{A} in equation (15)) can be assessed by comparing them with their supply side counterpart. In this context, a high degree of similarity indicates an insufficient coverage of demand factors to explain the

price dependencies. To this purpose, we use the cross-price matrices of the demand side ($\tilde{\mathcal{A}}$) and the supply side ($\tilde{\Gamma}$) and evaluate their similarities. We do this following Gandy and Veraart (2019) and consider the following standard criteria

$$(17) \quad \text{Sensitivity} = \frac{1}{\mu} \sum_{i=1}^n \sum_{j=1}^n \mathbb{1}_{\{\tilde{\alpha}_{ij} \neq 0\}} \cdot \mathbb{1}_{\{\tilde{\gamma}_{ij} > 0\}}$$

$$(18) \quad \text{Specificity} = \frac{1}{n^2 - \mu} \sum_{i=1}^n \sum_{j=1}^n \mathbb{1}_{\{\tilde{\alpha}_{ij} = 0\}} \cdot \mathbb{1}_{\{\tilde{\gamma}_{ij} = 0\}}$$

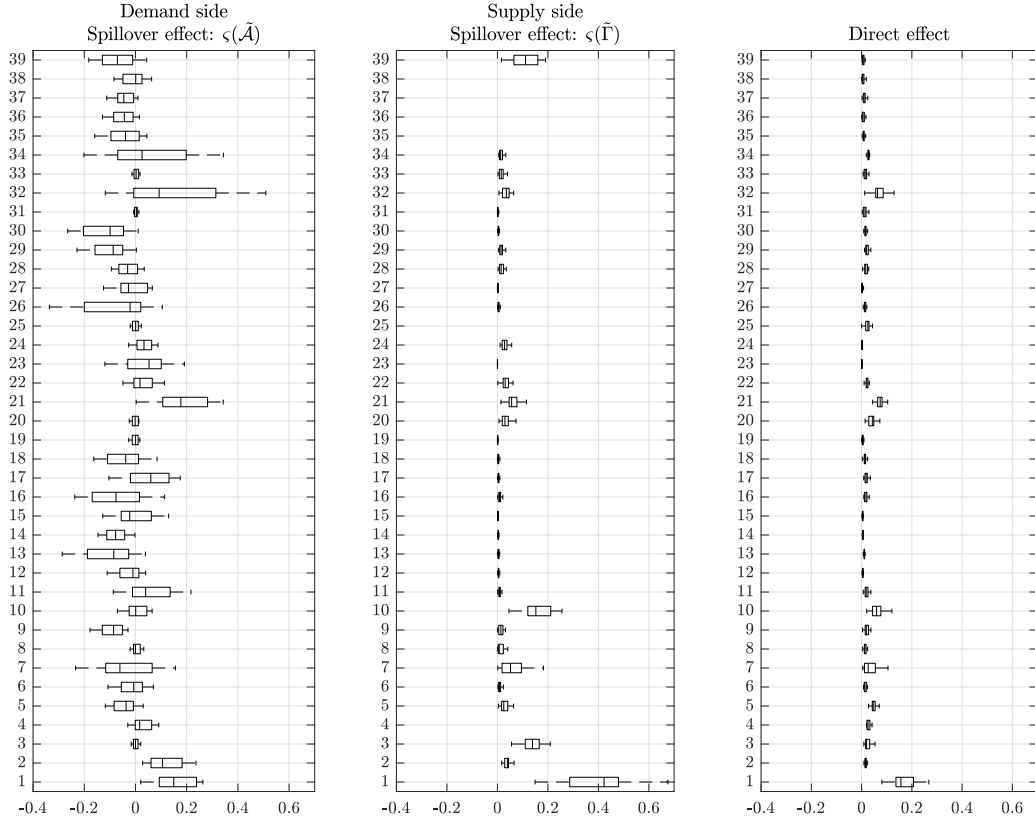
$$(19) \quad \text{Accuracy} = \frac{1}{n^2} \sum_{i=1}^n \sum_{j=1}^n (\mathbb{1}_{\{\tilde{\alpha}_{ij} = 0 \wedge \tilde{\gamma}_{ij} = 0\}} + \mathbb{1}_{\{\tilde{\alpha}_{ij} \neq 0 \wedge \tilde{\gamma}_{ij} > 0\}})$$

$$(20) \quad \text{Cosine-Similarity} = \frac{\sum_{i=1}^n \sum_{j=1}^n \tilde{\alpha}_{ij} \tilde{\gamma}_{ij}}{\sqrt{\sum_{i=1}^n \sum_{j=1}^n \tilde{\alpha}_{ij}^2} \sqrt{\sum_{i=1}^n \sum_{j=1}^n \tilde{\gamma}_{ij}^2}}$$

where, as before, $\mathbb{1}_{\{\cdot\}}$ is the indicator function and $\mu = \sum_{i=1}^n \sum_{j=1}^n \mathbb{1}_{\{\tilde{\gamma}_{ij} > 0\}}$. The first three criteria are in the range $[0, 1]$, and higher values indicate a greater extent of similarity, while the fourth is in the range $[-1, 1]$, with a higher value (in amount) indicating a higher extent of similarity. The results are provided in Table 2. The low value of the sensitivity measure indicates a markedly low congruence between the two adjacency matrices ($\tilde{\mathcal{A}}$ for the demand-driven and $\tilde{\Gamma}$ for the supply-driven cross-price networks) with respect to the non-zero entries. This shows, on the one hand, that sufficient supply variables have been included in the estimation to separate the demand- and supply-driven influences on the cross-price dependencies, and, on the other hand, that the cross-price dependencies from the estimation of the matrix $\tilde{\mathcal{A}}$ in equation (15) can indeed be interpreted as the result of demand-specific influences. The moderate value of the specificity measure is due to the fact that both cross-price networks are rather sparse, giving rise to only a small number of non-zero edges (consider the link density in Table 2). The accuracy measure, as a combination of the previous two, confirms the low congruence of the two adjacency matrices. Finally, the cosine-similarity measure again has a markedly low value, which is due to the low overall congruence of the two adjacency matrices with respect to their non-zero edges on the one hand, and on the other hand, to the fact that once a non-zero edge applies to the same element i, j in the two adjacency matrices, the sign of these entries can be different which augments their dis-similarities even further.

3.3. The empirical spillover effects. The network representation in Figure 2 shows the links, their signs and the corresponding node connections, but does not allow a quantitative assessment of individual price shocks on the CPI inflation rate. Moreover, given the differences between the demand- and supply-driven cross-price dependencies,

FIGURE 3. Individual price shocks: Direct and spillover effects



Note: The box-plots show the variation across countries of (i) the spillover effects, and (ii) the direct effects of a shock to an individual price subindex to the CPI inflation rate. The direct effects (DE) are given by $\pi^{\text{DE}} = \mathbf{w}'\mathbf{u}$ (this just reflects the weights of the price subindices in the CPI) and the spillover effects by equation (10). In each box, the central marker indicates the median, and the lower and upper edges of the box indicate the 25th and 75th percentiles of the cross-country variation, respectively. The whiskers extend to the most extreme non-outlying data points.

the question arises as to what extent the resulting spillover effects of microeconomic price shocks on the CPI inflation rate differ. A quantification of the spillover effects and a comparison between the demand- and supply-driven network of cross-price dependencies is the focus of what follows.

In line with the second column of Table 1, we compute the spillover effects of the individual price subindices on the CPI inflation rate. Technically, this is done by again using equation (10) where we set each element in the vector of shocks \mathbf{u} equal to zero except its i 's element which has a unit entry ($u_i = 1$). This allows us to calculate the spillover effect of a shock to the subindex of price i on the CPI inflation rate. We do this for each price subindex. The results are provided in the first panel of Figure 3 in the form of box-plots showing the variation across countries. The figure highlights a few noteworthy things.

First, there is a remarkable cross-country variation in the sign and quantitative magnitude of the spillover effects. Consider, for instance, the price subindex No. 1 (food)

in the left-hand panel. The median value of the spillover effect of this subindex is 0.15 implying that a one percentage point increase of this subindex raises the CPI inflation rate by 0.15 percentage points; the values for the boxes (25th and 75th percentiles) are 0.09 and 0.23, respectively, which undermine the large cross-country differences. The finding of a significant extent of heterogeneity in the spillover effects across countries aligns with the results put forth in Abdallah and Kpodar (2023) who focus on the role of retail energy prices for the CPI.

Second, the spillover effects from the supply-driven network (second panel of Figure 3) are always non-negative because of the solely positive valued edges while those from the demand-driven counterpart can be either negative or positive. Thus, while microeconomic price shocks can only be exacerbated by supply-driven cross-price dependencies, demand-driven cross-price dependencies can lead to an attenuation or exacerbation of the same shocks. This is particularly evident in the case of the price subindex No. 39 (other services n.e.c.), where a large positive (median) value of the supply-driven network of cross-price dependencies contrasts with a large negative (in amount) value of the demand-driven counterpart. In a similar vein, the extent of shock exacerbation is likely to be especially pronounced in the case of the price subindices No. 1 (food), 21 (operation of personal transport equipment) and 32 (catering), as in each case positive valued spillover effects result from both the demand- and supply-driven cross-price dependencies.

Third, on average, the size of the spillover effect of the price subindices exceeds their direct effect (right-hand panel in Figure 3; they reflect the weights of the price subindices in the CPI) on the CPI inflation rate. This is the case for both the demand- and the supply-driven cross-price networks. For the latter, the extent of asymmetry is especially pronounced for the price subindices No. 1 (food), 3 (alcoholic beverages), 10 (electricity, gas and other fuels) and 39 (other services n.e.c.). This highlights the importance of the spillover effects relative to the direct effects in explaining the impact of microeconomic price shocks on the CPI inflation rate.

4. THE ROLE OF CROSS PRICE DEPENDENCIES FOR INFLATION DYNAMICS

The previous section has highlighted the role of the cross-price dependencies for the size and sign of the spillover effects of microeconomic price shocks on the CPI inflation rate. This raises the question of whether they also matter for the overall inflationary dynamics.

With a view to equation (6), the inflation rate is determined by two elements. On the one hand, there are the exogenous shocks \mathbf{u} . In the theoretical model in Section 2, supply was assumed to be inelastic with respect to the price, so that demand shocks were the only element shaping prices and hence the CPI inflation rate. In a more general setting, however, the vector \mathbf{u} can contain any exogenous shock. On the other hand, the inflation rate in equation (6) depends on the extent of cross-price dependencies, which are governed by the price-Jacobian matrix \mathcal{A} . The cross-price dependencies determine the size and sign of the spillover effects. For a given vector of shocks \mathbf{u} , changes in the price-Jacobian matrix alter the spillover effects and hence the inflation rate. This motivates considering the CPI inflation rate π as a function $f(\cdot)$ of (i) the exogenous shock elements in \mathbf{u} and (ii) the spillover effects $\varsigma_{\mathcal{A}} \in \mathbb{R}$ that emerge from the price-Jacobian matrix \mathcal{A}

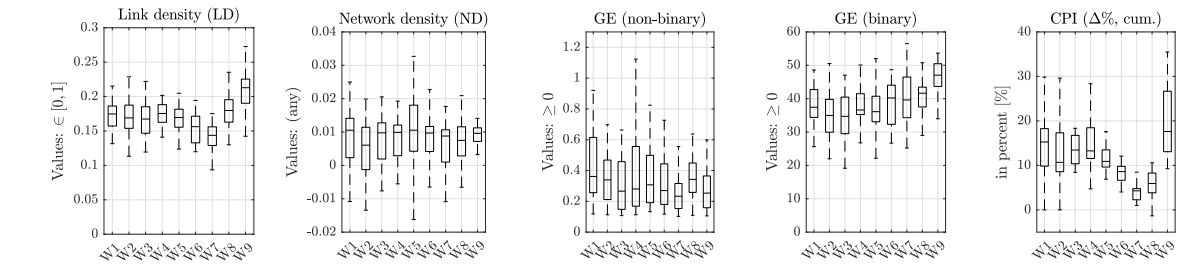
$$(21) \quad \pi = f(\varsigma_{\mathcal{A}}, u)$$

where the vector of shocks \mathbf{u} has been reduced to the scalar u for simplicity. Importantly, the spillover effects $\varsigma_{\mathcal{A}}$ are determined by the strength and the diffusion effect, both of which were discussed in Section 2.3. To get a better insight into the role of the spillover effects on the CPI inflation rate, we consider a second-order Taylor approximation of equation (21) around $u_0 = 0$, which yields the following

$$(22) \quad \pi = f_{\varsigma_{\mathcal{A}}} \cdot \tilde{\varsigma}_{\mathcal{A}} + f_u \cdot u + \frac{1}{2} (f_{\varsigma_{\mathcal{A}}\varsigma_{\mathcal{A}}} \cdot (\tilde{\varsigma}_{\mathcal{A}})^2 + f_{uu} \cdot (u)^2 + f_{\varsigma_{\mathcal{A}}u} \cdot \tilde{\varsigma}_{\mathcal{A}}u)$$

where $\tilde{\varsigma}_{\mathcal{A}} = \varsigma_{\mathcal{A}} - \varsigma_{\mathcal{A},0}$ and $f(\varsigma_{\mathcal{A}}, 0) = 0$. The spillover effects $\varsigma_{\mathcal{A}}$ thus shape the inflation rate along two dimensions. The first of these comes from the first-order terms and holds whenever $f_{\varsigma_{\mathcal{A}}} = \partial\pi/\partial\varsigma_{\mathcal{A}} \neq 0$. The effects of this term can be considered as an extension of the weights \mathbf{w} of the individual price subindices for the CPI. For given values of u , changes in it will affect the CPI inflation rate. The second dimension is comparatively more important and emerges from the second-order terms. The main focus here is on the term $f_{\varsigma_{\mathcal{A}}u}$. It determines the propagation mechanism of the exogenous shocks u . It applies whenever $f_{\varsigma_{\mathcal{A}}u} = \partial^2\pi/\partial u\partial\varsigma_{\mathcal{A}} \neq 0$, given that $f_u = \partial\pi/\partial u \neq 0$. Intuitively, changes in consumer preferences are likely to alter the structure of the cross-price dependencies, which in turn causes changes to the propagation mechanism of microeconomic price shocks to the CPI inflation rate. In what follows, we examine both dimensions. To do so, we approximate the spillover effects $\varsigma_{\mathcal{A}}$ by the network topology measures put forth in Section 2.4.

FIGURE 4. Network topology measures: country and time variation



Note: The box-plots show the variation across countries and time of the network topology measures. They are based on a window estimation of equation (15), with each window having a length of 60 months. The CPI inflation rate is given by the cumulative relative change for each window.

4.1. First-order terms. We enter the first-order terms of equation (22) into a panel data regression model in which we explain the CPI inflation rate by the spillover effects ς_A and the shocks \mathbf{u} . We proxy the spillover effects by the network topology ($\text{NT}(\tilde{\mathcal{A}})$) measures (link density, network density and graph energy) as motivated in Section 2.4. For the shock elements \mathbf{u} , we use the variables of a classical Philips curve specification, namely: the producer price index (PPI), the cyclical unemployment gap (U-Gap)¹³ and the import price index (IMPI) (see Aguiar and Martins, 2005; Hazell et al., 2022, and the references therein). We create an appropriate time variation of the network (compare Holme and Saramäki, 2012) by estimating equation (15) over different time windows of 60 months each, with an overlap to obtain estimates for a total of nine windows. We use the adjacency matrix $\tilde{\mathcal{A}}_{c,t}$ of each window $t = 1, \dots, 9$ to compute the network topology measures and we do this for each country $c = 1, \dots, 28$. Figure 4 shows the variation over time and across countries of the three network topology measures and the CPI inflation rate (cumulative relative change). There is a remarkable variation across countries in the three network topology measures and the CPI inflation rate, as is indicated by the width of the boxes. At the same time, there is also a strong variation over time, best illustrated by the temporal variation of the median estimate. This is the case for both the CPI inflation rate and the network topology measures.

We estimate a panel data regression model of the form

$$(23) \quad \pi_{c,t} = \beta_{\text{NT}} \cdot \text{NT}(\tilde{\mathcal{A}}_{c,t}) + \sum_{i=1}^K \beta_i x_{c,t,i} + e_{c,t}$$

to explain the CPI inflation rate $\pi_{c,t}$. As regards equation (23), the $K = 3$ explanatory variables ($x_{c,t,i}$) next to the network topology measure $\text{NT}(\tilde{\mathcal{A}}_{c,t})$ are given by the producer price index (PPI), the unemployment gap (U-Gap) and the import price index

¹³The unemployment gap (U-Gap) is measured by the cyclical component of the monthly year-over-year change in unemployment, extracted using the Hodrick-Prescott filter with a smoothing parameter of 14,400 (Ravn and Uhlig, 2002).

(IMPI), $e_{c,t}$ is the error term, c denotes the country and t the time variation. The temporal variation t is limited to the nine time windows. All variables are based on a monthly frequency. The price variables (CPI, PPI, IMPI) enter in cumulative percentage changes for the respective time windows and the unemployment gap enters as level.

We use the fixed effects (FE) estimator as it is considered to be the adequate approach for a situation where there are unobservable country effects and unobservable time effects. The results are provided in Table 3, where we report the estimates of distinct specifications of equation (23) (Reg. 1 to Reg. 6). The first regression (Reg. 1) does not include any of the network topology measures and the estimates for the partial effects of the remaining explanatory variables (PPI, U-Gap, IMPI) are in each case statistically significantly different from zero at least at the one percent level and all parameter estimates have their expected signs. For example, the estimates indicate, that a one percentage point increase in the producer price inflation rate leads to an increase in the CPI inflation rate of 0.14 percentage points; this partial effect turns out higher in the case of import prices (0.24). The remaining regressions (Reg. 2 to 6) include the network topology measures.

In a sequential extension of the basic regression model (Reg. 1) to include the network topology measures, we find that, first, link density (Reg. 2) is statistically significant in explaining the CPI inflation rate. This confirms the importance of cross-price dependencies for the CPI inflation rate in general. At the same time, however, we find that the network density (Reg. 3) has less statistical support for explaining the variation in the CPI inflation rate. Looking at Figure 4, this is not surprising, especially as this topology measure exhibits a lower extent of time variation. Most importantly, this measure captures changes in the connectedness along both the strength and diffusion effects. While link density has indicated the significant role of the diffusion effect, network density implies that both effects apply. The fact that the statistical significance level is slightly lower than for the link density suggests that the strength effect moderates the overall effect to some extent.

Finally, the graph energy (Reg. 4 and Reg. 5) has a high explanatory power for the CPI inflation rate. This is the case for both measures ($GE_{\mathbb{Z}_2}$ and $GE_{\mathbb{R}}$). Although the coefficient estimate of the binary graph energy measure ($GE_{\mathbb{Z}_2}$) is small, this should not obscure the importance of this variable, especially as its values are high (see Figure 4). The fact that the graph energy measures have a statistically significant impact on the inflation rate highlights the role of cyclical interdependencies between the price subindices

TABLE 3. Network topology measures and the CPI inflation rate

	First-order Taylor approximation					Second-order Taylor approximation					
	Reg. 1	Reg. 2	Reg. 3	Reg. 4	Reg. 5	Reg. 6	Reg. 7	Reg. 8	Reg. 9	Reg. 10	Reg. 11
	Dependent variable: CPI inflation rate ^(a)										
LD	-	0.44**	-	-	-	0.01	-	1.00	-	-	-
ND	-	-	15.31*	-	-	16.66**	-	-	5.28	-	-
GE _{Z₂}	-	-	-	0.00***	-	0.00*	-	-	-	-0.00	-
GE _R	-	-	-	-	0.29**	0.35***	-	-	-	-	0.44*
PPI ^(a)	0.14***	0.13***	0.14***	0.13***	0.14***	0.13***	0.39***	-0.17	0.04**	0.06	0.07*
U-Gap ^(b)	-3.25***	-3.08***	-2.88***	-3.11***	-3.27***	-2.71***	-2.70***	-2.72***	-2.29***	-2.57***	-2.61***
IMPI ^(a)	0.24***	0.27***	0.24***	0.28***	0.23***	0.27***	0.13***	0.18***	0.14***	0.20***	0.12***
LD · PPI	-	-	-	-	-	-	-	2.66***	-	-	-
ND · PPI	-	-	-	-	-	-	-	-	26.43*	-	-
GE _{Z₂} · PPI	-	-	-	-	-	-	-	-	-	0.01***	-
GE _R · PPI	-	-	-	-	-	-	-	-	-	-	0.97*
(LD) ²	-	-	-	-	-	-	-	-3.50	-	-	-
(ND) ²	-	-	-	-	-	-	-	-	-679	-	-
(GE _{Z₂}) ²	-	-	-	-	-	-	-	-	-	0.00	-
(GE _R) ²	-	-	-	-	-	-	-	-	-	-	0.11
(PPI) ²	-	-	-	-	-	-	-0.25***	-0.17***	-0.24***	-0.20***	-0.26***
R ²	0.31	0.33	0.32	0.34	0.33	0.35	0.44	0.56	0.52	0.55	0.54

Notes: The table reports the results from a panel data fixed effects regression model. The acronyms refer to link density (LD), network density (ND) and graph energy (GE) for the network topology measures and producer price index (PPI), unemployment gap (U-Gap) and import price index (IMPI) for the remaining explanatory variables. For each regression, the number of observations is $N \cdot T = 252$ with $T = 9$ and $N = 28$. The asterisks refer to the following levels of statistical significance: *** for 1 percent, ** for 5 percent and * for 10 percent.

^(a) The inflation rates of the CPI, PPI and IMPI are measured as the cumulative change within each time-window.

^(b) The unemployment gap (U-Gap) is measured by the cyclical component of the year-over-year change in unemployment, extracted using the Hodrick-Prescott filter with a smoothing parameter of 14,400.

(see Table 1). Cyclical interdependencies imply that the effects of microeconomic price shocks are slow to dissipate, resulting in long-lasting effects of microeconomic price shocks on the CPI inflation rate.

When all four network topology measures are used simultaneously in the regression model (Reg. 6), most of the measures retain their statistical properties. However, in the case of the two graph energy measures and the link density, we observe a slight decrease of these properties which is due to multicollinearity, as the link density and the two graph energy measures are positively correlated with each other.

4.2. Second-order terms. We now extend the panel data regression model given by equation (23) to include the second-order terms of equation (22). We estimate the extended model again using the fixed effects estimator and provide the results in the last five columns (Reg. 7 to Reg. 11) of Table 3. We restrict the interaction terms to the producer price index and the four network topology measures, since in all other cases the results are not statistically significant. In these five cases, however, the second-order terms provide several interesting results and insights.

The results highlight that in all cases (Reg. 7 to 11) the unemployment gap (U-Gap) and the import price inflation rate (IMPI) keep their high level of statistical significance compared to the estimation results of the first-order terms, but in each case their partial effects are noticeably lower than in the first-order terms set-up. As regards the producer price index (PPI), both the first-order terms and the quadratic terms are of statistical importance (consider Reg. 7) and the partial effect is given by $\frac{\partial \pi}{\partial PPI} = 0.32$ (the mean value of the PPI was used: $\overline{PPI} = 0.15$), which exceeds that of the first-order terms model. We ignore the second-order terms of the unemployment gap and the import price inflation rate since in each case the parameter estimates are not statistically different from zero.

When the network topology measures (Reg. 8 to Reg. 11) are added, the quadratic term of the PPI loses its high level of statistical significance in some cases. The partial effect of the producer price index $\partial \pi / \partial PPI$ is now given by 0.26 for Reg. 8, 0.23 for Reg. 9, 0.26 for Reg. 10 and 0.28 for Reg. 11, when using the mean values for the relative change in the producer price index ($\overline{PPI} = 0.15$), the link density ($\overline{LD} = 0.18$), the network density ($\overline{ND} = 0.01$) and the graph energy measures ($\overline{GE_{Z_2}} = 38.5$ and $\overline{GE_{\mathbb{R}}} = 0.3$). In each case, the partial effects are slightly larger than those of the model containing only the first-order terms (Reg. 1 to Reg. 6).

Most importantly, however, we find that the terms for $f_{\varsigma_A u}$ in equation (22), given by $\frac{\partial^2 \pi}{\partial PPI \partial LD} = 2.66$, $\frac{\partial^2 \pi}{\partial PPI \partial ND} = 26.43$, $\frac{\partial^2 \pi}{\partial PPI \partial GE_{Z_2}} \approx 0.01$ and $\frac{\partial^2 \pi}{\partial PPI \partial GE_{\mathbb{R}}} = 0.97$ from the

panel data regression results are all positive. Moreover, these parameter values are all statistically different from zero. This implies that the transmission mechanism of changes in the producer prices to the CPI inflation rate are shaped by the demand-driven cross-price dependencies. More specifically, a higher link density (LD) and/or a higher (binary) graph energy ($GE_{\mathbb{Z}_2}$) exacerbates any change in the producer prices on the CPI inflation rate. In these two cases, the extent of shock exacerbation occurs only due to the diffusion effect. In the case of the link density, the diffusion arises from the increase in the number of links between prices, which raises the overall degree of connectedness. In the case of the (binary) graph energy, diffusion results from the occurrence of additional cycles between prices, which means that the effect of a shock is slow to dissipate. However, as highlighted by the network density (ND) and non-binary graph energy measure ($GE_{\mathbb{R}}$), the strength effect is also important alongside to the diffusion effect, although the statistical support is weaker for these topology measures. This suggests that the strength effect attenuates the diffusion effect which is due to the negative valued edges. This in turn reflects the substitutive relationships between goods.

These results demonstrate the importance of the second-order terms of the cross-price dependencies and their important role in shaping the propagation mechanism of shocks to the CPI inflation rate. This is supported by the goodness-of-fit measure (R^2): while the regressors explain up to 35 percent of the variation in the CPI inflation rate in the model containing only the first-order terms, this rises to 56 percent when the second-order terms are added. The interaction terms contribute a major part to this increase.

4.3. Further remarks. The results presented here are robust to various extensions in form of additional variables being used in equation (15) to estimate the network of cross-price dependencies, different specifications of the prior densities for the empirical price-Jacobian matrix ($\tilde{\mathcal{A}}$), additional explanatory variables in the panel data regression model in equation (23), both for the version of the first-order terms and also for the second-order terms, and when robust standard errors are used (no change in the significance levels). A detailed discussion of the robustness checks can be found in the Appendix, where we also consider extensions related to an assessment of the inflation risks based on the network topology measures within a quantile regression framework.

As a final note, we attempted to estimate equation (23) using the network topology measures based on the supply-driven cross-price dependencies ($\tilde{\Gamma}$). However, significant data limitations impaired the implementation. On the one hand, calibration is not

possible for some countries because I-O tables are not available. On the other hand, for many other countries, I-O tables are only available for a limited number of recent years. This confines both the time span and the country coverage rendering impossible a proper estimation of equation (23).

5. CONCLUSION

We assess the role of demand-driven links between prices for the CPI inflation rate. Since the links arise from the complementary and substitutive properties of goods, they can be either negative or positive. Based on a simple theoretical model, we highlight the role of the structure and sign of these links in shaping the spillover effects of microeconomic price shocks on the CPI inflation rate, giving rise to a strength and a diffusion effect. The former is determined by the size and sign of the cross-price dependencies, with spillover effects increasing with the size of positive valued links, while negative links can give rise to both mitigating and exacerbating effects. With regards to the diffusion effect, when goods are complements, the spillover effects increase with the number of links; moreover the presence of a link structure in the form of a cycle renders the amplification particularly pronounced.

We test the theoretical findings empirically by estimating demand-driven cross-price dependencies using a spatial econometric model. We use the three-digit subindices of the CPI for 28 countries (UK and current EU member states) and find that, first, positive valued links dominate, highlighting the relative importance of the complementarity property between goods. Second, the spillover effects of the price subindices on the CPI inflation rate are both negative and positive and their quantitative magnitude outweighs the direct effects in most cases. Third, demand-driven links between prices show remarkable differences from a supply side counterpart and tend to change over time, reflecting changes in consumer preferences.

Finally, we examine whether the structure of the cross-price dependencies also matters for overall inflation dynamics. We find that the cross-price dependencies themselves have a statistically significant impact on the CPI inflation rate, but, more importantly, they shape the impact of other variables (such as producer prices) on the CPI inflation rate. This empirical result is consistent with that of the theoretical model and highlights the role of the demand system in the transmission of microeconomic price shocks to the CPI inflation rate.

The results of this study shed light on the role of consumer preferences in the demand-driven diffusion of inflation. The complementary or substitutive nature of goods is key

in this respect, leading to a mitigation or exacerbation of microeconomic price shocks on the CPI inflation rate.

REFERENCES

- Abdallah, Chadi, and Kangni Kpodar (2023) ‘How large and persistent is the response of inflation to changes in retail energy prices?’ *Journal of International Money and Finance* 132, 102806
- Acemoglu, Daron, Vasco M. Carvalho, Asuman Ozdaglar, and Alireza Tahbaz-Salehi (2012) ‘The Network Origins of Aggregate Fluctuations.’ *Econometrica* 80(5), 1977–2016
- Afrouzi, Hassan, and Saroj Bhattarai (2022) ‘Inflation and GDP Dynamics in Production Networks: A Sufficient Statistics Approach.’ SSRN Working papers 4045782
- Aguiar, Alvaro, and Manuel Martins (2005) ‘Testing the significance and the non-linearity of the Phillips trade-off in the Euro Area.’ *Empirical Economics* 30(3), 665–691
- Ahmad, Yamin S., and Olena M. Staveley-O’Carroll (2017) ‘Exploring international differences in inflation dynamics.’ *Journal of International Money and Finance* 79, 115–135
- Asgharian, Hossein, Lu Liu, and Marcus Larsson (2018) ‘Cross-border asset holdings and comovements in sovereign bond markets.’ *Journal of International Money and Finance* 86(C), 189–206
- Auer, Johannes, and Dominik Papies (2020) ‘Cross-price elasticities and their determinants: a meta-analysis and new empirical generalizations.’ *Journal of the Academy of Marketing Science* 48(3), 584–605
- Auer, Raphael A., and Aaron Mehrotra (2014) ‘Trade linkages and the globalisation of inflation in Asia and the Pacific.’ *Journal of International Money and Finance* 49, 129–151
- Auer, Raphael A., and Philip Sauré (2013) ‘The globalisation of inflation: a view from the cross section.’ In *Globalisation and inflation dynamics in Asia and the Pacific*, ed. Bank for International Settlements, vol. 70 (Bank for International Settlements) pp. 113–118
- Auer, Raphael A., Andrei A. Levchenko, and Philip Sauré (2019) ‘International Inflation Spillovers through Input Linkages.’ *The Review of Economics and Statistics* 101(3), 507–521
- Balcilar, Mehmet, Ahmed H. Elsayed, and Shawkat Hammoudeh (2023) ‘Financial connectedness and risk transmission among MENA countries: Evidence from connectedness network and clustering analysis.’ *Journal of International Financial Markets, Institutions and Money* 82, 101656
- Bhattacharya, Anirban, Debdeep Pati, Natesh S. Pillai, and David B. Dunson (2015) ‘Dirichlet–Laplace priors for optimal shrinkage.’ *Journal of the American Statistical Association* 110(512), 1479–1490
- Bilgin, Nuriye Melisa (2022) ‘Inflation diffusion through production networks.’ SSRN Working papers 4164364
- Bilgin, Nuriye Melisa, and Kamil Yılmaz (2018) ‘Producer price inflation connectedness and input-output networks.’ SSRN Working papers 3244645
- Boccaletti, S., V. Latora, Y. Moreno, M. Chavez, and D.-U. Hwang (2006) ‘Complex networks: Structure and dynamics.’ *Physics Reports* 424(4), 175–308
- Brož, Václav, and Evžen Kočenda (2018) ‘Dynamics and factors of inflation convergence in the European union.’ *Journal of International Money and Finance* 86, 93–111
- Cai, Mattia, and Toon Vandyck (2020) ‘Bridging between economy-wide activity and household-level consumption data: Matrices for European countries.’ *Data in Brief* 30, 1–4
- Carrière-Swallow, Yan, Pragyant Deb, Davide Furceri, Daniel Jiménez, and Jonathan D. Ostry (2023) ‘Shipping costs and inflation.’ *Journal of International Money and Finance* 130, 102771
- Choi, Sangyup, Davide Furceri, Prakash Loungani, Saurabh Mishra, and Marcos Poplawski-Ribeiro (2018) ‘Oil prices and inflation dynamics: Evidence from advanced and developing economies.’ *Journal of International Money and Finance* 82, 71–96
- Colizza, V., A. Flammini, M. A. Serrano, and A. Vespignani (2006) ‘Detecting rich-club ordering in complex networks.’ *Nature Physics* 2(2), 110–115
- Das, Sanjiv R., Madhu Kalimipalli, and Subhankar Nayak (2022) ‘Banking networks, systemic risk, and the credit cycle in emerging markets.’ *Journal of International Financial Markets, Institutions and Money* 80, 101633
- Di Giovanni, Julian, and Andrei A. Levchenko (2010) ‘Putting the parts together: trade, vertical linkages, and business cycle comovement.’ *American Economic Journal: Macroeconomics* 2(2), 95–124
- Diewert, W. Erwin (2009) ‘Cost of living indexes and exact index numbers.’ In *Quantifying Consumer Preferences*, ed. D.J. Slottje (London: Emerald Group Publishing Limited, Bingley) chapter 8, pp. 207–245

- Elhorst, J. Paul, Marco Gross, and Eugen Tereanu (2021) ‘Cross-sectional dependence and spillovers in space and time: Where spatial econometrics and global VAR models meet.’ *Journal of Economic Surveys* 35(1), 192–226
- Fadinger, Harald, Christian Ghiglino, and Mariya Teteryatnikova (2022) ‘Income differences, productivity, and input-output networks.’ *American Economic Journal: Macroeconomics* 14(2), 367–415
- Fan, Tianlong, Linyuan Lü, Dinghua Shi, and Tao Zhou (2021) ‘Characterizing cycle structure in complex networks.’ *Communications Physics* 4(272), 1–9
- Frank, Ove, and Frank Harary (1982) ‘Cluster inference by using transitivity indices in empirical graphs.’ *Journal of the American Statistical Association* 77(380), 835–840
- Gandy, Axel, and Luitgard Anna Maria Veraart (2019) ‘Adjustable network reconstruction with applications to CDS exposures.’ *Journal of Multivariate Analysis* 172, 193–209
- Gefang, Deborah, Stephen G. Hall, and George S. Tavlas (2022) ‘Fast Two-Stage Variational Bayesian Approach to Estimating Panel Spatial Autoregressive Models with Unrestricted Spatial Weights Matrices.’ *arXiv preprint arXiv:2205.15420*
- Gelos, Gaston, and Yulia Ustyugova (2017) ‘Inflation responses to commodity price shocks – How and why do countries differ?’ *Journal of International Money and Finance* 72, 28–47
- Glasserman, Paul, and H. Peyton Young (2016) ‘Contagion in financial networks.’ *Journal of Economic Literature* 54(3), 779–831
- Gutman, Ivan (1978) ‘The energy of a graph.’ In ‘10. Steiermärkisches Mathematisches Symposium (Stift Rein, Graz, 1978),’ vol. 103 of *Ber. Math.-Statist. Sect. Forsch. Graz Austria* pp. 1–22
- Hall, Stephen G., George S. Tavlas, and Yongli Wang (2022) ‘Drivers and Spillover Effects of Inflation: the United States, the Euro Area, and the United Kingdom.’ *Journal of International Money and Finance* p. 102776
- Hall, Stephen G., George S. Tavlas, and Yongli Wang (2023) ‘Drivers and spillover effects of inflation: The United States, the euro area, and the United Kingdom.’ *Journal of International Money and Finance* 131, 102776
- Hazell, Jonathon, Juan Herreño, Emi Nakamura, and Jón Steinsson (2022) ‘The Slope of the Phillips Curve: Evidence from U.S. States.’ *Quarterly Journal of Economics* 137(3), 1299–1344
- Heil, Thomas L.A., Franziska J. Peter, and Philipp Prange (2022) ‘Measuring 25 years of global equity market co-movement using a time-varying spatial model.’ *Journal of International Money and Finance*
- Holland, Paul W., Kathryn Blackmond Laskey, and Samuel Leinhardt (1983) ‘Stochastic block models: First steps.’ *Social Networks* 5(2), 109–137
- Holme, Petter, and Jari Saramäki (2012) ‘Temporal networks.’ *Physics Reports* 519(3), 97–125
- Horvath, Steve (2011) *Weighted Network Analysis: Applications in Genomics and Systems Biology* SpringerLink: Bücher (Springer New York)
- IMF (2022a) ‘Calculating consumer price indices in practice.’ In ‘Consumer Price Index Manual’ (Washington, USA: International Monetary Fund, IMF) chapter 9, pp. 153–177
- (2022b) ‘The economic approach to index number theory: the many-household case.’ In ‘Consumer Price Index Manual’ (Washington, USA: International Monetary Fund, IMF) chapter 18, pp. 243–269
- Jalali, Neda, and Manoochehr Babanezhad (2011) ‘Quantile regression due to skewness and outliers.’ *Applied Mathematical Sciences* 5(39), 1947 – 1951
- Jehle, Geoffrey Alexander, and Philip J. Reny (2011) *Advanced microeconomic theory*, 3rd ed. (Harlow: Pearson Education)
- Karamysheva, Madina, and Ekaterina Seregina (2022) ‘Prudential policies and systemic risk: The role of interconnections.’ *Journal of International Money and Finance* 127(C), 1–22
- Karrer, Brian, and Mark E. J. Newman (2011) ‘Stochastic block models and community structure in networks.’ *Physical Review E* 83, 016107
- Kim, Hyun-Joo, and Jin Min Kim (2005) ‘Cyclic topology in complex networks.’ *Physical Review E* 72(3), 14–23
- Kleibergen, Frank, and Eric Zivot (2003) ‘Bayesian and classical approaches to instrumental variable regression.’ *Journal of Econometrics* 114(1), 29–72
- Lam, Clifford, and Pedro C.L. Souza (2020) ‘Estimation and selection of spatial weight matrix in a spatial lag model.’ *Journal of Business & Economic Statistics* 38(3), 693–710
- Mehta, Nitin, and Yu Ma (2012) ‘A multcategory model of consumers’ purchase incidence, quantity, and brand choice decisions: Methodological issues and implications on promotional decisions.’ *Journal of Marketing Research* 49(4), 435–451
- Mulhern, Francis J., and Robert P. Leone (1991) ‘Implicit price bundling of retail products: A multi-product approach to maximizing store profitability.’ *Journal of Marketing* 55(4), 63–76

- Neely, Christopher J., and David E. Rapach (2011) ‘International comovements in inflation rates and country characteristics.’ *Journal of International Money and Finance* 30(7), 1471–1490
- Newman, M. E. J. (2003) ‘Mixing patterns in networks.’ *Physical Review E* 67, 026126
- (2010) *Networks: an introduction* (Oxford; New York: Oxford University Press)
- Newman, M. E. J., and Juyong Park (2003) ‘Why social networks are different from other types of networks.’ *Physical Review E* 68, 036122
- Opsahl, Tore, Vittoria Colizza, Pietro Panzarasa, and José J. Ramasco (2008) ‘Prominence and control: The weighted rich-club effect.’ *Physical Review Letters*
- Pal, Amresh Bahadur, Ashutosh Kumar Dubey, and Anoop Chaturvedi (2016) ‘Shrinkage estimation in spatial autoregressive model.’ *Journal of Multivariate Analysis* 143, 362–373
- Peña, Ismael, and Juan Rada (2008) ‘Energy of digraphs.’ *Linear and Multilinear Algebra* 56(5), 565–579
- Pesaran, M. Hashem (2021) ‘General diagnostic tests for cross-sectional dependence in panels.’ *Empirical Economics* 60(1), 13–50
- Pesaran, M. Hashem, Til Schuermann, and Scott M. Weiner (2004) ‘Modeling regional interdependencies using a global error-correcting macroeconomic model.’ *Journal of Business & Economic Statistics* 22(2), 129–162
- Pfarrhofer, Michael (2022) ‘Modeling tail risks of inflation using unobserved component quantile regressions.’ *Journal of Economic Dynamics and Control* 143(C), 1–19
- Ravn, Morten, and Harald Uhlig (2002) ‘On adjusting the Hodrick-Prescott filter for the frequency of observations.’ *The Review of Economics and Statistics* 84(2), 371–375
- Regmi, Anita, and James L. Seale (2010) ‘Cross-Price Elasticities of Demand Across 114 Countries.’ Technical Bulletin 59870, United States Department of Agriculture, Economic Research Service, March
- Rossi, Peter E., Greg M. Allenby, and Robert MacCulloch (2006) *Bayesian statistics and marketing*, repr. with corr. ed. (Harlow: Hoboken, N.J. [u.a.]: Wiley)
- Sethuraman, Raj, V. Srinivasan, and Doyle Kim (1999) ‘Asymmetric and neighborhood cross-price effects: Some empirical generalizations.’ *Marketing Science* 18(1), 23–41
- Teteryatnikova, Mariya (2014) ‘Systemic risk in banking networks: Advantages of “tiered” banking systems.’ *Journal of Economic Dynamics and Control* 47, 186–210
- van Oest, Rutger (2005) ‘Which Brands Gain Share from Which Brands? Inference from Store-Level Scanner Data.’ *Quantitative Marketing and Economics* 3(1), 281–304
- Watts, Duncan J., and Steven H. Strogatz (1998) ‘Collective dynamics of ‘small-world’ networks.’ *Nature* 393(6684), 440–442
- Werner, Dirk (2009) ‘Funktionalanalysis.’ In ‘Einführung in die höhere Analysis’ (Berlin, Heidelberg: Springer) pp. 1–88
- Xu, Xiao-Ke, Jie Zhang, and Michael Small (2010) ‘Rich-club connectivity dominates assortativity and transitivity of complex networks.’ *Physical Review E*
- Zhang, Wenjun, Wei Li, and Weibing Deng (2021) ‘The characteristics of cycle-nodes-ratio and its application to network classification.’ *Communications in Nonlinear Science and Numerical Simulation* 99, 1–11

APPENDIX A. CROSS-PRICE EFFECTS FROM A SUPPLY SIDE VIEW

This section motivates price-dependencies arising from value chains along production networks. We follow Acemoglu et al. (2012) in this respect. Consider again a static economy with $n \in \mathbb{N}$ goods. We now assume that the demand by consumers for these n goods is perfectly price inelastic. Each good is produced in a distinct industry and can be either purchased by the consumers or used as an intermediate input for the production of other goods. Firms in each industry employ Cobb-Douglas production technologies with constant returns to scale to transform intermediate inputs and labor into final goods. In particular, the output of industry i is given by

$$(24) \quad x_i = \xi_i \Gamma_i^{\gamma_i} \prod_{j=1}^n x_{ij}^{\gamma_{ij}}$$

where l_i is the amount of labor hired by firms in industry i , $x_{ij} \in \mathbb{R}_+$ is the quantity of good j used for the production of good i , $\gamma_i > 0$ denotes the share of labor in industry i 's production technology and ξ_i is an industry specific productivity shock. The exponents $\gamma_{ij} \geq 0$ in equation (24) formalize the idea that firms in an industry may need to rely on the goods produced by other industries as intermediate inputs for production. Note that, in general, $\gamma_{ij} \neq \gamma_{ji}$ and $\gamma_i + \sum_{j=1}^n \gamma_{ij} = 1$. Firms in industry i choose their demand for labor and intermediate goods to maximize profits, $\pi_i = P_i x_i - l_i - \sum_{j=1}^n P_j x_{ij}$, while taking all prices (P_1, \dots, P_n) as given and the wage is normalized to one. The first-order conditions imply that $x_{ij} = \gamma_{ij} P_i x_i / P_j$ and $l_i = \gamma_i P_i x_i$. Plugging these expressions into firm i 's production function, equation (24), and taking logarithms implies that

$$(25) \quad \Delta p_i = \sum_{j=1}^n \gamma_{ij} \Delta p_j + \varepsilon_i$$

where $\varepsilon_i = -\Delta \log(\xi_i)$ and $p_i = \log(P_i)$. Since the above relationship has to hold for all industries $i = 1, \dots, n$, it provides a system of equations to solve for all relative prices in terms of productivity shocks. It can be rewritten in matrix form

$$(26) \quad \Delta \mathbf{p} = \mathbf{\Gamma} \cdot \Delta \mathbf{p} + \boldsymbol{\varepsilon}$$

where $\mathbf{\Gamma} = [\gamma_{ij}]_{i,j=1}^n$ is the economy's input-output matrix, $\mathbf{p} = [p_i]_{i=1}^n \in \mathbb{R}^n$ is again the price vector and $\boldsymbol{\varepsilon} = [\varepsilon_i]_{i=1}^n \in \mathbb{R}^n$ is a vector of supply shocks. Since demand is price inelastic, equilibrium prices are set by goods' supplies only according to equation (26). Consequently, the equilibrium CPI inflation rate is given by

$$(27) \quad \pi = \mathbf{w}'(I - \mathbf{\Gamma})^{-1} \boldsymbol{\varepsilon}$$

where the price level according to the CPI is given by $\log(p) = \mathbf{w}'\mathbf{p}$ and $\pi = \Delta \log(p) = \mathbf{w}'\Delta \mathbf{p}$. Equation (27) expresses the inflation rate in terms of industry-level shocks and the economy's production network. The latter captures the input-output (I-O) linkages between various industries and they are summarized in the matrix $\mathbf{\Gamma}$. From an empirical point of view, the I-O matrix of an economy as constructed by the national statistical offices and it is defined in terms of input expenditures as a fraction of sales, that is, $\eta_{ij} = P_j x_{ij} / P_i x_i$. However, in the special case that all technologies are Cobb-Douglas, η_{ij} coincides with the exponent γ_{ij} in equation (24).

Some remarks on the matrix $\mathbf{\Gamma}$ are in order. First, note that the assumption that $\gamma_i + \sum_{j=1}^n \gamma_{ij} = 1$ with $\gamma_i > 0$ implies that for all rows $i = 1, \dots, n$ in $\mathbf{\Gamma}$ we have that $\sum_{j=1}^n \gamma_{ij} < 1$. Following Werner (2009), this implies that the matrix $\mathbf{\Gamma}$ has a spectral radius $\varrho(\mathbf{\Gamma})$ that satisfies $0 < \varrho(\mathbf{\Gamma}) < 1$ which in turn guarantees that $I - \mathbf{\Gamma}$ is invertible and, moreover, the economy's Leontief inverse $\tilde{\mathcal{L}} = (I - \mathbf{\Gamma})^{-1}$ can be decomposed in form

of a Neumann-series: $\tilde{\mathcal{L}} = (I - \mathbf{\Gamma})^{-1} = \sum_{k=0}^{\infty} \mathbf{\Gamma}^k$. This implies that $\tilde{l}_{ij} = \gamma_{ij} + \sum_{h=1}^n \gamma_{ih} \gamma_{hj} + [\dots]$ where $\tilde{l}_{ij} \in \tilde{\mathcal{L}}$, with the first term in this expression accounting for industry j 's role as a direct intermediate goods' supplier to industry i , the second term accounting for j 's role as a supplier to i 's suppliers, and so on. Interpreted in terms of the production network representation of the economy, \tilde{l}_{ij} accounts for all possible directed walks (of various lengths) that connect industry j to industry i over the network. The latter in turn shapes the transmission of price shocks originating in specific industries on the CPI inflation rate.

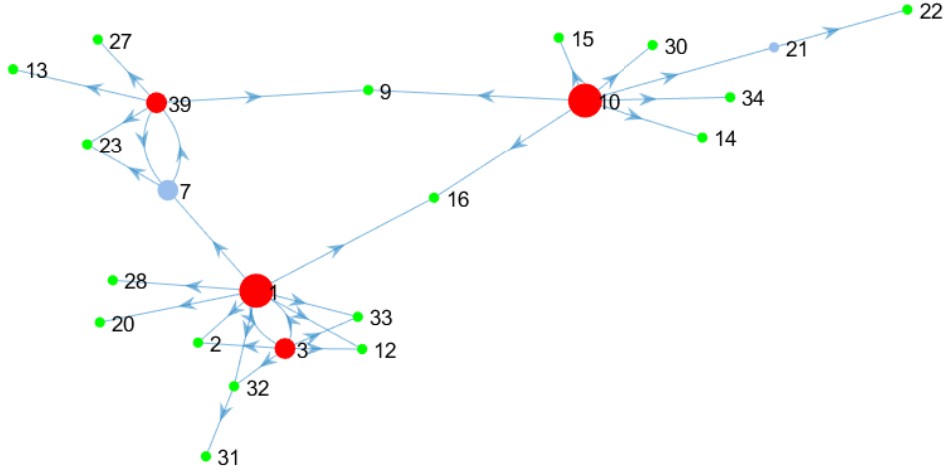
A.1. From the I-O to the COICOP (CPI) classification. In what follows, we examine the conversion of the production network $\mathbf{\Gamma}$ based on the I-O classification into the COICOP classification on which the CPI is based upon. This serves to enable a direct comparison of the two price networks given by \mathcal{A} and $\mathbf{\Gamma}$. We use the input-output (I-O) tables to this purpose. I-O tables can be product-by-product or industry-by-industry matrices combining both supply and use tables into a single matrix. We use the latter for our purposes. These tables depict inter-industry relationships within an economy, showing how output from one industry may become an input to another industry. They quantify the inter-industry relationships by means of a matrix. Their column entries capture inputs to an industry, while row entries represent outputs from a given industry. This arrangement, therefore, shows the extent of dependency of one industry on another, both as a customer of outputs from other industries and as a supplier of inputs. Industries may also depend on their own output, that is, on a portion of their own production; this is delineated by the entries of the main diagonal. Each column of the I-O matrix shows the monetary value of inputs to each sector and each row represents the value of each sector's outputs.

We convert the I-O classification into the COICOP classification on which the CPI is based upon by using the concordance matrices \mathbf{B} of Cai and Vandyck (2020). This gives rise to a production network expressed in terms of the COICOP classification which we denote by $\tilde{\mathbf{\Gamma}}$ and it is given by

$$(28) \quad \tilde{\mathbf{\Gamma}} = \mathbf{B}' \mathbf{\Gamma} \mathbf{B}$$

Equation (28) maps the production network based on the I-O classification into a new production network based on the COICOP classification. Moreover, the transformation in equation (28) makes sure that both matrices (\mathcal{A} from the demand (consumer) side and $\tilde{\mathbf{\Gamma}}$ from the supply (firm) side) have the same dimension ($n \times n$). This implies that the two price-Jacobian matrices can now be compared directly to each other.

FIGURE 5. I-O network based on the CPI classification (COICOP)



Note: The figure shows the production network given by the I-O tables based on the COICOP classification for which the concordance matrices of Cai and Vandyck (2020) were used. The network shown is the average over all countries (the UK and the current EU member countries). We only show the edges that are greater than 0.01. Nodes in red indicate out-degree dominance while those in green in-degree dominance; nodes in blue indicate equality between out- and in-degree.

A.2. Price dependencies from the supply side. We collect the I-O tables (Γ) for the UK and the current EU member countries for the year 2015 which allows for the highest data coverage across countries; no I-O tables are available for Bulgaria and Luxembourg. The classification which these tables are based upon is outlined in Table 5 in the Appendix. We re-classify the tables by using the concordance matrices of Cai and Vandyck (2020) which map the I-O tables (Γ) based on the I-O classification (Table 5) into the COICOP classification (Table 4) by using equation (28). This yields $\tilde{\Gamma}$. We re-classify the matrix $\tilde{\Gamma}$ in line with the assumptions of equation (24) and the constraint that $\gamma_i + \sum_{j=1}^n \gamma_{ij} = 1$ where we set the labor share γ_i equal to 0.45 for each sector $i = 1, \dots, n$ (Acemoglu et al., 2012). This implies that the elements $\tilde{\gamma}_{ij} \in \tilde{\Gamma}$ satisfy $0 \leq \tilde{\gamma}_{ij} < 1 \forall i, j = 1, \dots, n$. We then compute the average of $\tilde{\Gamma}$ across all countries in our sample and show the corresponding production network in Figure 5. We omit self-loops and use size-thresholding to enable a better visual inspection. The size-thresholding applies to the value of the edges $\tilde{\gamma}_{ij}$ and we omit all those edges which are less than 0.01 in value. This gives rise to a link density equal to 33 percent, see Table 2. Note that the price network Γ as of the production network does not need to be estimated as it was the case for the price network \mathcal{A} as of the consumer demand side. This is due to the fact that the I-O tables identify the links (edges) of the network (compare Bilgin and Yilmaz, 2018).

The resulting network shown in Figure 5 has some interesting characteristics. First of all, the prices associated with the nodes (prices) 1, 3, 7, 10 and 39 act as the central sources of shocks in the network. In each case the out-degree clearly predominates over the in-degree (nodes in red). While the interaction among themselves is limited, they in turn shape the dynamics of a series of other prices (nodes) which are connected to these five central prices. This particular network structure gives rise to a disassortative network (negative degree-correlation, see Table 2). Secondly, the network is characterized by rich dynamics, since a cycle applies twice involving on the one hand prices No. 1 and 3 and prices No. 7 and 39 on the other hand. This can also be seen by the high value of the graph energy (GE) measures as provided in Table 2. Third, the network gives rise to three blocks and can hence be considered as a *stochastic block model* (Holland et al., 1983; Karrer and Newman, 2011). The first involves the prices in the upper-left corner of Figure 5 with prices No. 7 and 39 as the central ones; the second block is given by the prices in the right part of the figure involving price No. 10 as the central one, and finally, the third block is comprised by the prices in the lower-left corner involving prices No. 1 and 3 as the central ones.

APPENDIX B. ECONOMETRIC FRAMEWORK

We consider a panel model with N cross-sectional and T time observations of the form:

$$(29) \quad \mathbf{y}_t = \mathbf{A}\mathbf{y}_t + \mathbf{X}_t\boldsymbol{\beta} + \boldsymbol{\varepsilon}_{yt},$$

where \mathbf{y}_t is an N by 1 vector of the dependent variable measured at time $t = 1, \dots, T$. \mathbf{X}_t is an $N \times Q$ matrix of explanatory variables with corresponding slope parameter vector $\boldsymbol{\beta}$.

Network effects are governed by the unknown ($N \times N$) matrix \mathbf{A} , with zero on the main diagonal ($a_{ii} = 0$ for all i). In the spatial econometrics literature the term $\mathbf{A}\mathbf{y}_t$ is called a spatial lag, where endogeneity may be addressed by using instruments for the spatial lag. We therefore use an $N \times N$ matrix $\underline{\mathbf{A}}$, which comprises prior knowledge on \mathbf{A} , along with Dirichlet-Laplace shrinkage priors (Bhattacharya et al., 2015) to avoid over-parameterization. Our model set-up is thus a Bayesian Markov chain Monte-Carlo (MCMC) version reminiscent to recent work by Gefang et al. (2022) and Lam and Souza (2020). For estimation of \mathbf{A} , we follow Lam and Souza (2020) and construct instruments from within the model by interacting the expert prior information $\underline{\mathbf{A}}$ with

the exogenous variables. The $(N \times P)$ matrix of instruments \mathbf{Z}_t thus contains vectors from the matrix $[\mathbf{X}_t, \underline{\mathbf{A}}\mathbf{X}_t, \underline{\mathbf{A}}^2\mathbf{X}_t, \dots]$.¹⁴

Defining the endogenous spatial lag $\bar{\mathbf{y}}_t = \mathbf{A}\mathbf{y}_t$ the equation for the spatial lag can be written as:

$$(30) \quad \bar{\mathbf{y}}_t = \mathbf{Z}_t\boldsymbol{\delta} + \boldsymbol{\varepsilon}_{\bar{\mathbf{y}}t}.$$

After vertically stacking the dependent variable and the respective design matrices T times (and thus removing the time subscript), equations (30) and (29) can be written as:

$$(31) \quad \bar{\mathbf{y}} = \mathbf{Z}\boldsymbol{\delta} + \boldsymbol{\varepsilon}_{\bar{\mathbf{y}}}$$

$$(32) \quad \mathbf{y} = \bar{\mathbf{y}} + \mathbf{X}\boldsymbol{\beta} + \boldsymbol{\varepsilon}_y,$$

where $\bar{\mathbf{y}} = (\mathbf{I}_T \otimes \mathbf{A})\mathbf{y}$ and $\boldsymbol{\delta}$ is a P dimensional column parameter vector. Equations (31) and (32) denote the structural form of a system of equations with a single endogenous variable and multiple instruments \mathbf{Z} , where $[\boldsymbol{\varepsilon}_{\bar{\mathbf{y}},i}, \boldsymbol{\varepsilon}_{y,i}]' \sim \mathcal{N}(\mathbf{0}, \boldsymbol{\Sigma})$. The

reduced-form errors are obtained using the transformation of the structural errors via

$$\begin{bmatrix} \nu_{\bar{\mathbf{y}},i} \\ \nu_{y,i} \end{bmatrix} = \begin{bmatrix} 1 & 0 \\ 1 & 1 \end{bmatrix} \begin{bmatrix} \boldsymbol{\varepsilon}_{\bar{\mathbf{y}},i} \\ \boldsymbol{\varepsilon}_{y,i} \end{bmatrix}.$$

For Markov-chain Monte Carlo (MCMC) estimation we elicit standard conditional conjugate priors on the unknown parameters along with a Dirichlet-Laplace shrinkage prior (Bhattacharya et al., 2015) on the unknown off-diagonal elements in \mathbf{A} . We follow Rossi et al. (2006) and Kleibergen and Zivot (2003), among several others, and put an inverted Wishart prior on the structural error variance component $\boldsymbol{\Sigma}$, $p(\boldsymbol{\Sigma}) \sim \mathcal{IW}(\underline{\nu}, \underline{\mathbf{S}})$, where the (scalar) $\underline{\nu}$ and the (2×2) matrix $\underline{\mathbf{S}}$ contain prior hyperparameters. For the slope parameter of the two equations, normal priors are used, $p(\boldsymbol{\beta}) \sim \mathcal{N}(\underline{\boldsymbol{\mu}}_{\boldsymbol{\beta}}, \underline{\mathbf{V}}_{\boldsymbol{\beta}})$ and $p(\boldsymbol{\delta}) \sim \mathcal{N}(\underline{\boldsymbol{\mu}}_{\boldsymbol{\delta}}, \underline{\mathbf{V}}_{\boldsymbol{\delta}})$. Similar to recent work by Gefang et al. (2022), who put forward a variational Bayes approach for estimation of the (off-diagonal) elements in \mathbf{A} , we employ a Dirichlet-Laplace (DL) shrinkage prior advocated by Bhattacharya et al. (2015). The DL prior set-up comprises hierarchical global and local shrinkage parameters and is

¹⁴However, it is worth noting that in case of using no prior information ($\underline{\mathbf{A}} = \mathbf{0}$), no spatial lags of the explanatory variables can be computed and the elements in \mathbf{A} are shrunk towards a sparse matrix.

structured for the elements a_{ij} for $i \neq j$ as follows:

$$(33) \quad p(a_{ij}) \sim \mathcal{N}(\underline{a}_{ij}, \tau^2 \varphi_{ij}^2 \psi_{ij}^2)$$

$$(34) \quad \tau \sim \mathcal{G}(N(N-1)\underline{c}, 1/2)$$

$$(35) \quad \psi_{ij} \sim \text{Exp}(1/2)$$

$$(36) \quad \boldsymbol{\varphi} \sim \text{Dir}(\underline{c}, \dots, \underline{c}).$$

where the matrix $\underline{\mathbf{A}}$ with typical element \underline{a}_{ij} represents the prior mean (or expert information) of the network structure \mathbf{A} . The prior of the local shrinkage parameters ψ_{ij} are exponentially distributed and uses a vector of scales to provide flexibility on the shrinkage process. The prior on the vector $\boldsymbol{\varphi}$, which collects all individual φ_{ij} , is Dirichlet distributed where the prior hyperparameter \underline{c} governs the prior tightness.

B.1. Markov chain Monte-Carlo estimation. This subsection describes the Bayesian MCMC sampler employed. After eliciting suitable prior hyperparameters, the MCMC sampling algorithm makes inference of a set of draws from the conditional posterior distributions of the unknown parameters after discarding a first set of draws as burn-ins. Given the conditional conjugate prior set-up we can set up a standard Gibbs sampler by producing draws from the conditional posterior distributions.

Updating $\boldsymbol{\beta}$. Sampling the slope parameters in a Gibbs sampler is straightforward since conditional on all other parameters the errors $\boldsymbol{\varepsilon}_{\bar{y}}$ can be treated as observable, too:

$$(37) \quad \begin{aligned} y_i &= \bar{y}_i + \mathbf{x}'_i \boldsymbol{\beta} + \varepsilon_{y,i} | \varepsilon_{\bar{y},i} \\ &= \bar{y}_i + \mathbf{x}'_i \boldsymbol{\beta} + \frac{\Sigma_{12}}{\Sigma_{11}} \varepsilon_{\bar{y},i} + \nu_{y|\bar{y}}. \end{aligned}$$

Using the laws of conditional distributions, note that $\text{var}(\nu_{y|\bar{y}}) = \Sigma_{22} - \Sigma_{12} \Sigma_{11}^{-1} \Sigma_{21}$, the equation can be simply transformed to a standard Bayesian regression problem with a standard normal error. This results in a Gaussian conditional posterior such that a standard Gibbs sampling step can be employed.

Updating $\boldsymbol{\delta}$. We can sample from the conditional posterior for $\boldsymbol{\delta}$, by using the reduced form representation of the model:

$$(38) \quad \bar{y}_i = \mathbf{z}'_i \boldsymbol{\delta} + \varepsilon_{\bar{y},i}$$

$$(39) \quad y_i - \mathbf{x}'_i \boldsymbol{\beta} = \mathbf{z}'_i \boldsymbol{\delta} + (\varepsilon_{\bar{y},i} + \varepsilon_{y,i})$$

Note that $\text{var} \begin{pmatrix} \varepsilon_{\bar{y},i} \\ \varepsilon_{\bar{y},i} + \varepsilon_{y,i} \end{pmatrix} = \begin{bmatrix} 1 & 0 \\ 1 & 1 \end{bmatrix} \boldsymbol{\Sigma} \begin{bmatrix} 1 & 1 \\ 0 & 1 \end{bmatrix} = \mathbf{L}' \mathbf{L}$, where the upper triangular 2 by 2 matrix \mathbf{L} can be computed using Cholesky factorization. The equation above can be

transformed to a regression model with standard normal errors by pre-multiplication with $(\mathbf{L}^{-1})'$. The resulting representation can be written as:

$$(40) \quad (\mathbf{L}^{-1})' \begin{bmatrix} \bar{y}_i \\ y_i - \mathbf{x}'_i \boldsymbol{\beta} \end{bmatrix} = (\mathbf{L}^{-1})' \begin{bmatrix} \mathbf{z}'_i \\ \mathbf{z}'_i \end{bmatrix} \boldsymbol{\delta} + \mathcal{N}(\mathbf{0}, \mathbf{I}_2)$$

Equation (40) can be used to set up a standard Gaussian sampling step for $\boldsymbol{\delta}$ with a doubled number of observations.

Updating $\boldsymbol{\Sigma}$. The conditional posterior distribution of $\boldsymbol{\Sigma}$ is well-known and has an inverted Wishart form:

$$(41) \quad p(\boldsymbol{\Sigma} | \bullet, \mathcal{D}) \sim \mathcal{IW}(NT + \underline{\nu}, \mathbf{S} + \underline{\mathbf{S}})$$

$$\mathbf{S} = \begin{bmatrix} \boldsymbol{\varepsilon}'_{\bar{y}} \\ \boldsymbol{\varepsilon}'_y \end{bmatrix} \begin{bmatrix} \boldsymbol{\varepsilon}'_{\bar{y}} \\ \boldsymbol{\varepsilon}'_y \end{bmatrix}'$$

Updating the shrinkage parameters and the prior variance for \mathbf{A} . The hierarchical global-local shrinkage parameters and thus the prior variance for \mathbf{A} as defined in equation (44) are updated according to Bhattacharya et al. (2015). The respective parameters can be updated by sampling from their conditional posterior distribution using the generalized inverse Gaussian (GIG) distribution:

$$(42) \quad p(\tilde{\psi}_{ij} | \boldsymbol{\varphi}, \mathbf{A}) \sim \text{GIG}(-1/2, 1, \mu_{\varphi_{ij}}^{-2}),$$

where $\mu_{\varphi_{ij}} = \varphi_{ij} \tau / |a_{ij}|$ and after drawing from the conditional posterior we set $\psi_{ij} = 1/\tilde{\psi}_{ij}$. The global shrinkage parameter τ is also sampled from a GIG using

$$(43) \quad p(\tau | \boldsymbol{\varphi}_{ij}, \mathbf{A}) \sim \text{GIG}\left(1 - N(N-1), 2 \sum_{i \neq j} \sum_{j \neq i} (|a_{ij} - \underline{a}_{ij}|) / \varphi_{ij}, 1\right).$$

In a last step, $\boldsymbol{\varphi}$ is updated using $N(N-1)$ auxiliary variables \tilde{w}_{ij} , with $\tilde{w}_{ij} \sim \text{GIG}(\underline{c} - 1, 2(|a_{ij} - \underline{a}_{ij}|), 1)$. After independently sampling all \tilde{w}_{ij} , we set φ_{ij} equal to $\tilde{w}_{ij} / \sum \tilde{w}_{ij}$. Subsequently, the (diagonal) prior variance covariance matrix for sampling the elements in \mathbf{A} can be updated according to equation (33).

Updating the elements in \mathbf{A} . Let \mathbf{E} denote an $(N \times T)$ matrix which comprises the reorganized $(NT \times 1)$ errors $\mathbf{y} - \mathbf{X}\boldsymbol{\beta}$ by T and N , and \mathbf{Y} is the respective $N \times T$ matrix of dependent variables. For the l th cross-section (i.e. the l th row vector of \mathbf{E} , \mathbf{e}_l),

$$(44) \quad \mathbf{e}'_l = \mathbf{Y}'_{-l} \mathbf{a}_{-l} + \boldsymbol{\nu}_{y|\bar{y}}$$

where \mathbf{e}'_l is $T \times 1$, \mathbf{Y}'_{-l} is $T \times (N-1)$ and \mathbf{a}_{-l} is $(N-1) \times 1$. As before, the $T \times 1$ vector $\boldsymbol{\nu}_{y|\bar{y}}$ has mean zero and diagonal variance Σ_{22} . Using equation (44), the elements of \mathbf{A}

can be updated row-wise equation by equation via a Gaussian distribution with prior variances updated from using the shrinkage parameters.

In practice, however, it is not a priori clear whether ignoring the endogeneity will lead to a bias in the results. In the context of the literature on global vector autoregressions (GVAR) (Pesaran et al., 2004), for example, the spatial lag is often assumed to be weakly exogenous, which is due to the “smallness condition”, which in turn ensures that all spatial units receive small enough weight to not exert a dominant unit structure (Pesaran et al., 2004; Pesaran, 2021). A detailed discussion is provided by Elhorst et al. (2021).

APPENDIX C. ROBUSTNESS AND EXTENSIONS

We consider various robustness checks which concern both the estimation of the demand-driven cross-price dependencies, additional network topology measures to capture the spillover effects that emanate from the network structure and finally the role of the skewness of the CPI inflation rate (and several explanatory variables) for the results. In what follows we address each aspect.

C.1. Alternative prior densities. We consider an alternative specification of the prior densities in the form of variations in the parameterization. In what follows, we elaborate on this in more detail. We do so since the choice of the prior density can have an impact on the (posterior) estimates obtained from a spatial econometric model.

The main results are based on a shrinkage prior. In general, as highlighted by Pal et al. (2016), shrinkage priors can be a useful tool for incorporating prior information and reducing estimation uncertainty in spatial econometric models. The main idea behind a shrinkage prior is to “shrink” or pull the estimates of the parameters towards a certain known value or distribution. This can help to reduce estimation uncertainty and improve the stability of the model. We considered the estimates provided in Regmi and Seale (2010) for the baseline results. They provide estimates for the cross-price dependencies for low-, middle-, and high-income countries. We relied on the low- and high-income country results for our baseline results. Here we consider two extensions. The first concerns a decomposition of the countries of our sample into three groups (low-, middle-, and high income countries), while the second considers a shrinkage towards zero in each case.

We decompose the 28 countries in our sample into three income groups (low, middle and high) based on the level of PPP-adjusted GDP per capita of the year 2021 and

we allocate an equal number of countries to each group. This implies that the low-income countries are: Bulgaria, Greece, Croatia, Romania, Latvia, Slovakia, Portugal, Hungary, Poland, Estonia; the middle-income countries are: Lithuania, Spain, Czech Republic, Cyprus, Slovenia, Italy, United Kingdom, France, Malta; and finally, the high income countries are given by: Finland, Belgium, Germany, Sweden, Austria, the Netherlands, Denmark, Ireland, Luxembourg. Each group is assigned the corresponding parameter estimates as of Table 4 in Regmi and Seale (2010) and the spatial econometric model is then re-estimated for each country. With a view to the results provided in Table 3 we find that there are no qualitative changes. Moreover, also the network statistics provided in Table 2 change only slightly. We interpret the results of this robustness check as a confirmation of our baseline results.

The second robustness check in this context concerns a shrinkage of the values in the matrix \mathbf{A} towards zero. We apply this calibration of the shrinkage prior to each country in our sample and again re-estimate the spatial econometric model and in turn all network topology measures for each country. We again find that there are no qualitative changes to the results provided in Table 3 of the panel data regression models, most importantly, also the significance pattern of the estimated parameters remains unchanged. We find though changes to the network statistics relative to those of the baseline results provided in Table 2. In particular, with the shrinkage prior that pushes the parameter estimates towards zero, the link density now has a lower value (0.18) and so too the (binary) graph energy (8.31), while the network density declines only slightly. Despite these changes to the network statistics, we consider these results again in favor of the stability and plausibility of the baseline results.

C.2. Additional explanatory variables. The estimation of the cross-price dependencies (\mathbf{A}) in equation (15) uses a series of exogenous variables (\mathbf{X}_t) to control for exogenous influences, in particular, supply side factors. In what follows we check for the stability of the estimates of the adjacency matrix $\tilde{\mathbf{A}}$ that emerges from the matrix \mathbf{A} by the statistical thresholding as defined in equation (16). To this purpose, we extend the list of exogenous variables in \mathbf{X}_t and re-estimate \mathbf{A} , $\tilde{\mathbf{A}}$ and the network topology measures for each country, to then re-run the panel data regression models as of equation (23). We consider labor market specific variables (employment growth rate, the unemployment rate), real activity measures (growth rate of retail trade and the industrial production index), financial market variables (growth rate of the stock market index, realized stock market volatility (based on a GARCH(1,1) model), yield curve on government bonds), further commodity and energy prices (corn, wheat, iron,

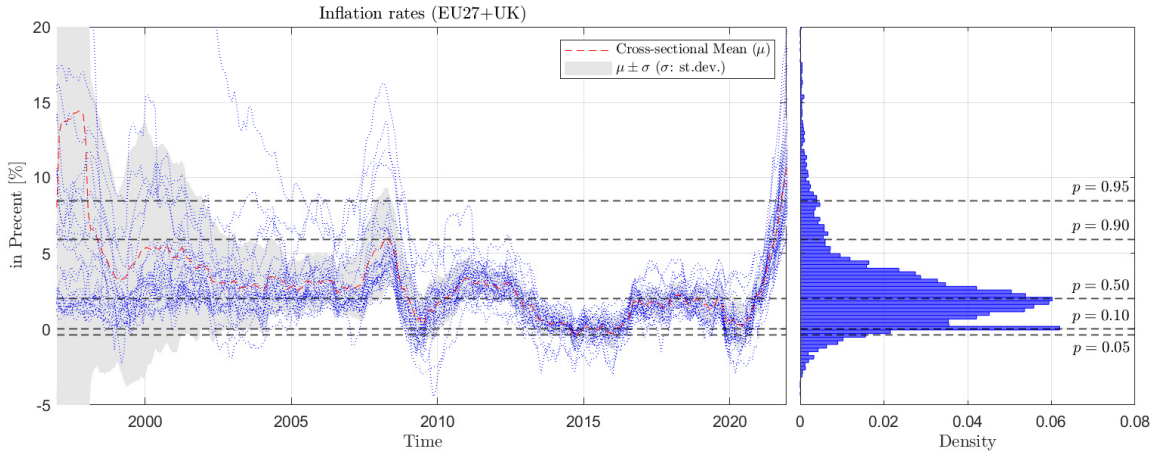
wood, electricity). We add each of these variables into the baseline model one by one and re-estimate the parameters of the model each time. In doing so, we determine the network topology measures each time and estimate the panel data regression model of equation (23) each time as a final step. We find that the results put forth in Table 3 hold qualitatively and conclude that our results are robust to extensions in the vector of the exogenous variables (\mathbf{X}_t).

In a second extension in this context, we employ our baseline results for the estimated price-Jacobian matrix \mathbf{A} and the corresponding adjacency matrix $\tilde{\mathbf{A}}$ and consider additional exogenous variables in the panel data regression model of equation (23) only. We consider the nominal effective exchange rate, unit labor costs, GDP, the money supply (M1), and labor market conditions such as the labor force participation rate and the number of job vacancies. Each of these variables is used in annual growth rates (except the labor force participation rate) and implement a temporal disaggregation to a monthly frequency, if necessary, using the method of Chow-Lin. We examined these variables solely in the first-order set-up in equation (23) to assess the differences of the parameter estimates of the network topology measures relative to those of the baseline results. We find that there are no qualitative changes to the results provided in Table 3 of the panel data regression models, most importantly, also the significance pattern of the estimated parameters remains unchanged. It has to be noted, though, at this point that the comparison is impaired to some extent by the fact that the country coverage is limited in some cases since not all countries provide (long) time series on vacancies, unit labor costs and alike.

C.3. Additional network topology measures. We challenge the baseline results with various additional network topology measures. This is important in our context since we utilize network topology measures to proxy for the spillover effects that emerge from the extent of network connectedness. To this purpose we consider the following additional measures: (i) transitivity, (ii) rich-club metric, and (iii) assortativity.

With a view to the network structure as provided in Figure 2, Xu et al. (2010) stress the importance of high-degree nodes for the structure of a complex system. This is commonly referred to as transitivity (“rich-club” phenomenon) and has been discussed in several instances in both social and computer sciences and refers to the tendency of high-degree nodes—the hubs of the network—to be very well connected to each other. For example, the clustering coefficient (Watts and Strogatz, 1998) is used to measure the transitivity property of a network. If a social network has a high clustering coefficient, it means that the “friends” of someone are also likely to be “friends” themselves (Newman

FIGURE 6. Inflation series: distribution over time and across countries



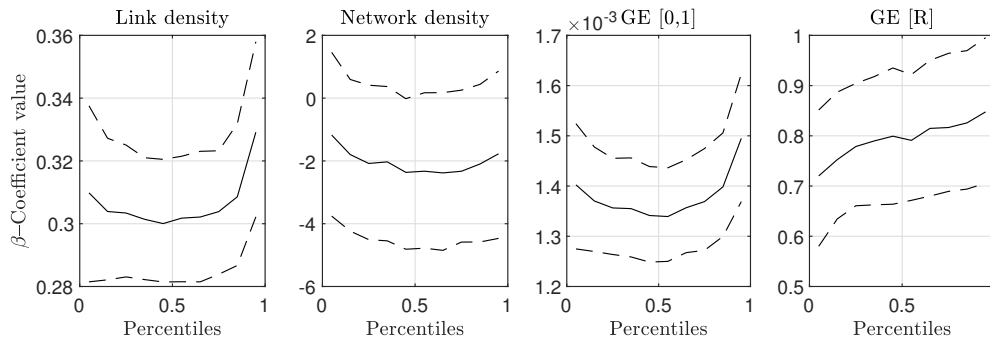
Note: The figures shows the year-over-year change in percent of the CPI index of the UK and the current EU member countries. The histogram in the right panel displays the distribution across countries and over time.

and Park, 2003). It is calculated by the ratio between the observed number of closed triplets and the maximum possible number of closed triplets in the graph. However, the clustering coefficient ignores the extent of interaction among high-degree nodes. To this purpose, Opsahl et al. (2008) extended the rich-club metric (Colizza et al., 2006) to take the tightness among connected nodes into account. Finally, the (dis-) assortativity is yet another measure in this context (Newman, 2003). It captures the preference for a network's nodes to attach to others that are (dis-) similar in some way.

We use each of these alternative network topology measures at a time instead of the ones in Table 3. We find that all of these three measures have a statistically significant first-order effect on the CPI inflation rate. The level of statistical significance is particularly high in case of the rich-club metric (<0.005). This highlights the role of the high-degree nodes in shaping the network structure, the overall network connectedness and hence the size (and sign) of the spillover effects of microeconomic price shocks on the CPI inflation rate.

C.4. Inflation risks. The choice of a mean framework in the regression analysis is not always appropriate for two reasons. First, when the distribution of a variable is highly skewed, and second when sever outliers are observed in the analysis. In contrast, quantile regression, in special case median regression, remains informative in such situations (Jalali and Babanezhad, 2011). Figure 6 provides some visual evidence of inflation skewness. In this context Brož and Kočenda (2018) stress the inflation convergence in the European Union and highlight that it became more widespread after the global financial crisis. As can be seen in Figure 6, the distribution of the inflation rates of the countries in our sample gives rise to a strongly left-skewed distribution (see

FIGURE 7. Quantile regression for first-order Taylor approximation



Note: The sub-panels show the parameter estimates of equation (23) based on a (Bayesian) quantile regression set-up. Each of the four network topology measures was used individually in the regression equation to avoid problems related to multicollinearity. The four panels show the parameter estimates of the network topology measures from the respective regression across the percentiles.

also Pfarrhofer, 2022). A similar extent of skewness applies to several of the control variables, as for instance the producer price inflation rate. Against this background, we now examine the effects of the price-network effects within a quantile regression framework. To this purpose we estimate equation (23) based on a quantile regression set-up and show the estimates across a range of the percentiles of the distribution of the explanatory variables. We limit the analysis to the first-order effects.

Each of the four network topology measures was used individually in the regression equation to avoid problems related to multicollinearity. The four panels in Figure 7 show the parameter estimates of the network topology measures from the respective regression. The figure shows the parameter estimates for the partial effect of the four network topology measures (link density, network density and the two graph energy measures) across their percentiles. The estimates of the link density highlight that the partial effect increase noticeably when the extent of links is particularly large. The same applies for the number of cycles which is expressed by the graph energy measures—a larger number of cycles gives rise to large spillover effects as the effect of microeconomic price shocks are only slow to dissipate. As a consequence, the overall effect of the graph energy measures on the CPI inflation rate are higher the larger the values of the graph energy measures are. In all cases, however, the statistical support is limited. This is due to the small amount of data points at the tails of the distributions.

APPENDIX D. ADDITIONAL FIGURES AND TABLES

TABLE 4. The three-digit subindices of the CPI (COICOP classification)

ID	Description
1	cp.011 Food
2	cp.012 Non-Alcoholic Beverages
3	cp.021 Alcoholic Beverages
4	cp.022 Tobacco
5	cp.031 Clothing
6	cp.032 Footwear
7	cp.041 Actual Rentals for Housing
8	cp.043 Maintenance and Repair of the Dwelling
9	cp.044 Water Supply and Miscellaneous Services Relating to the Dwelling
10	cp.045 Electricity, Gas and Other Fuels
11	cp.051 Furniture and Furnishings, Carpets and Other Floor Coverings
12	cp.052 Household Textiles
13	cp.053 Household Appliances
14	cp.054 Glassware, Tableware and Household Utensils
15	cp.055 Tools and Equipment for House and Garden
16	cp.056 Goods and Services for Routine Household Maintenance
17	cp.061 Medical Products, Appliances and Equipment
18	cp.062 Out-Patient Services
19	cp.063 Hospital Services
20	cp.071 Purchase of Vehicles
21	cp.072 Operation of Personal Transport Equipment
22	cp.073 Transport Services
23	cp.081 Postal Services
24	cp.082 Telephone and Telefax Equipment
25	cp.083 Telephone and Telefax Services
26	cp.091 Audio-Visual, Photographic and Information Processing Equipment
27	cp.092 Other Major Durables for Recreation and Culture
28	cp.093 Other Recreational Items and Equipment, Gardens and Pets
29	cp.094 Recreational and Cultural Services
30	cp.095 Newspapers, Books and Stationery
31	cp.096 Package Holidays
32	cp.111 Catering Services
33	cp.112 Accommodation Services
34	cp.121 Personal Care
35	cp.123 Personal Effects N.E.C.
36	cp.124 Social Protection
37	cp.125 Insurance
38	cp.126 Financial Services N.E.C.
39	cp.127 Other Services N.E.C.
Not used:	
–	cp.101 Pre-Primary and Primary Education
–	cp.102 Secondary Education
–	cp.103 Post-Secondary Non-Tertiary Education
–	cp.104 Tertiary Education
–	cp.105 Education Not Definable by Level

TABLE 5. The I-O tables: Classification

ID	Description
1 CPA_A01	Products of agriculture, hunting and related services
2 CPA_A02	Products of forestry, logging and related services
3 CPA_A03	Fish and other fishing products; aquaculture products; support services to fishing
4 CPA_B	Mining and quarrying
5 CPA_C10-12	Food, beverages and tobacco products
6 CPA_C13-15	Textiles, wearing apparel, leather and related products
7 CPA_C16	Wood and of products of wood and cork, except furniture; articles of straw and plaiting materials
8 CPA_C17	Paper and paper products
9 CPA_C18	Printing and recording services
10 CPA_C19	Coke and refined petroleum products
11 CPA_C20	Chemicals and chemical products
12 CPA_C21	Basic pharmaceutical products and pharmaceutical preparations
13 CPA_C22	Rubber and plastic products
14 CPA_C23	Other non-metallic mineral products
15 CPA_C24	Basic metals
16 CPA_C25	Fabricated metal products, except machinery and equipment
17 CPA_C26	Computer, electronic and optical products
18 CPA_C27	Electrical equipment
19 CPA_C28	Machinery and equipment n.e.c.
20 CPA_C29	Motor vehicles, trailers and semi-trailers
21 CPA_C30	Other transport equipment
22 CPA_C31-32	Furniture and other manufactured goods
23 CPA_C33	Repair and installation services of machinery and equipment
24 CPA_D	Electricity, gas, steam and air conditioning
25 CPA_E36	Natural water; water treatment and supply services
26 CPA_E37-39	Sewerage services; sewage sludge; waste collection, treatment and disposal services; materials recovery services; remediation services and others
27 CPA_F	Constructions and construction works
28 CPA_G45	Wholesale and retail trade and repair services of motor vehicles and motorcycles
29 CPA_G46	Wholesale trade services, except of motor vehicles and motorcycles
30 CPA_G47	Retail trade services, except of motor vehicles and motorcycles
31 CPA_H49	Land transport services and transport services via pipelines
32 CPA_H50	Water transport services
33 CPA_H51	Air transport services
34 CPA_H52	Warehousing and support services for transportation
35 CPA_H53	Postal and courier services
36 CPA_I	Accommodation and food services
37 CPA_J58	Publishing services
38 CPA_J59-60	Motion picture, video and television programme production services, sound recording and music publishing; programming and broadcasting services
39 CPA_J61	Telecommunications services
40 CPA_J62-63	Computer programming, consultancy and related services; Information services
41 CPA_K64	Financial services, except insurance and pension funding
42 CPA_K65	Insurance, reinsurance and pension funding services, except compulsory social security
43 CPA_K66	Services auxiliary to financial services and insurance services
44 CPA_L68	Real estate services
45 CPA_M69-70	Legal and accounting services; services of head offices; management consultancy services
46 CPA_M71	Architectural and engineering services; technical testing and analysis services

TABLE 5. The I-O tables: Classification

ID	Description
47 CPA_M72	Scientific research and development services
48 CPA_M73	Advertising and market research services
49 CPA_M74-75	Other professional, scientific and technical services and veterinary services
50 CPA_N77	Rental and leasing services
51 CPA_N78	Employment services
52 CPA_N79	Travel agency, tour operator and other reservation services and related services
53 CPA_N80-82	Security and investigation services; services to buildings and landscape; office administrative, office support and other business support services
54 CPA_O	Public administration and defence services; compulsory social security services
55 CPA_P	Education services
56 CPA_Q86	Human health services
57 CPA_Q87-88	Residential care services; social work services without accommodation
58 CPA_R90-92	Creative, arts, entertainment, library, archive, museum, other cultural services; gambling and betting services
59 CPA_R93	Sporting services and amusement and recreation services
60 CPA_S94	Services furnished by membership organisations
61 CPA_S95	Repair services of computers and personal and household goods
62 CPA_S96	Other personal services
63 CPA_T	Services of households as employers; undifferentiated goods and services produced by households for own use